Azole resistance is mediated by integration of sterol gene regulation and membrane transporter production by the zinc cluster-containing transcription factor Upc2A in *Candida glabrata*

Bao Gia Vu[1], Mark A. Stamnes[1], Yu Li[2], P. David Rogers[2,3] and W. Scott Moye-Rowley[1,*]

Running title: Upc2A global transcriptional regulation

From: [1]Department of Molecular Physiology and Biophysics, Carver College of Medicine, University of Iowa, Iowa City, IA 52242 USA; [2]Department of Clinical Pharmacy and Translational Science, University of Tennessee Health Science Center, Memphis, TN 38163 USA.

[3]Current Address: Department of Pharmaceutical Sciences, St. Jude Children's Hospital, Memphis, TN 38105-3678 USA.

[*]Corresponding author. E-mail: scott-moye-rowley@uiowa.edu

Draft: May 7, 2021

Abstract (300 words)

The most commonly used antifungal drugs are the azole compounds that interfere with biosynthesis of the fungal-specific sterol: ergosterol. The pathogenic yeast *Candida glabrata* commonly acquires resistance to azole drugs like fluconazole via mutations in a gene encoding a transcription factor called *PDR1*. These *PDR1* mutations lead to overproduction of drug transporter proteins like the ATP-binding cassette transporter Cdr1. In other *Candida* species, mutant forms of a transcription factor called Upc2 are associated with azole resistance, owing to the important role of this protein in control of expression of genes encoding enzymes involved in the ergosterol biosynthetic pathway. Recently, the *C. glabrata* Upc2A factor was demonstrated to be required for normal azole resistance, even in the presence of a hyperactive mutant form of *PDR1*. Using genome-scale approaches, we define the network of genes bound and regulated by Upc2A. By analogy to a previously described hyperactive *UPC2* mutation found in *Saccharomyces cerevisiae*, we generated a similar form of Upc2A in *C. glabrata* called G898D Upc2A. Chromatin immunoprecipitation coupled with Next Generation Sequencing (ChIP-seq) demonstrated that wild-type Upc2A binding to target genes was strongly induced by fluconazole while G898D Upc2A bound similarly, irrespective of drug treatment. We also carried out RNA-seq analysis to determine the genes that were direct or indirect targets of Upc2A transcriptional control. In addition to the well-described *ERG* genes as Upc2A transcriptional targets, we found a large group of genes encoding components of the translational apparatus along with membrane proteins. These Upc2A-regulated membrane protein-encoding genes are often targets of the Pdr1 transcription factor, demonstrating the high degree of overlap between these

two regulatory networks. Finally, we provide evidence that Upc2A impacts the Pdr1-Cdr1 system during the anaerobic response and also modulates resistance to caspofungin. These studies provide a new perspective of Upc2A as a master regulator of lipid and membrane protein biosynthesis.

Author summary (200 words)

In the pathogenic yeast *Candida glabrata*, expression of the genes encoding enzymes in the ergosterol biosynthetic pathway is controlled by the transcription factor Upc2A. *C. glabrata* has a low intrinsic susceptibility to azole therapy and acquires fluconazole resistance at high frequency. These azole resistant mutants typically contain substitution mutations in a gene encoding the transcription factor Pdr1. Pdr1 does not appear to regulate ergosterol genes and instead induces expression of genes encoding drug transport proteins like *CDR1*. Here we establish that extensive overlap exists between the regulatory networks defined by Upc2A and Pdr1. Genomic approaches are used to describe the hundreds of genes regulated by Upc2A that far exceed the well-described impact of this factor on genes involved in ergosterol biosynthesis. The overlap between Upc2A and Pdr1 is primarily described by co-regulation of genes encoding membrane transporters like *CDR1*. We provide evidence that Upc2A impacts the transcriptional control of the *FKS1* gene, producing a target of a second major class of antifungal drugs, the echinocandins. Our data are consistent with Upc2A playing a role as a master regulator coordinating the synthesis of membrane structural components, both at the level of lipids and proteins, to produce properly functional biological membranes.

Introduction

An almost inescapable problem for chemotherapy of microbes is the development of resistance. This problem is especially acute in the case of pathogenic fungi for which only 3 different drug classes exist for use in treatment of infections (reviewed in (1, 2)). The most commonly used drug class is the azole compounds, chief among these is the well-tolerated fluconazole (reviewed in (3)). Fluconazole targets ergosterol biosynthesis and has been used successfully since the 1980s but this success has led to the development of resistant organisms (recently discussed in (4)). The prevalence of fluconazole as an anti-Candidal therapy has likely contributed to the changing epidemiology of candidemias with the frequency of these fungal infections being increasingly associated with *Candida glabrata*; an increase that correlates with the introduction of fluconazole as an antifungal drug (5).

C. glabrata exhibits two features that complicate its control by fluconazole. First, this pathogen has a high intrinsic resistance to fluconazole (6). Second, high level resistant isolates easily arise that contain gain-of-function (GOF) mutations in a transcription factor-encoding gene called *PDR1* (7-9). The GOF *PDR1* alleles exhibit high levels of target gene expression and drive robust fluconazole resistance primarily through induction of expression of the ATP-binding cassette transporter-encoding gene *CDR1* (10, 11).

The primary species associated with candidemias is *Candida albicans* which can also acquire fluconazole resistance (recently discussed in (12)). Interestingly, the range of genes in which mutations are observed to associate with fluconazole resistance in *C.*

93 *albicans* is much wider than in *C. glabrata*. Along with mutant forms of the genes
94 encoding the well-described transcription factors Tac1 and Mrr1 (13, 14), two additional
95 genes in which fluconazole resistant alleles can emerge in *C. albicans* are *ERG11* (15),
96 that encodes the enzymatic target of azole drugs, and Upc2, the primary transcriptional
97 activator of *ERG11* and other ergosterol biosynthetic pathway genes (16). Mutations in
98 the cognate genes for these proteins have not been found in *C. glabrata*.
99 Two important observations have recently linked *C. glabrata* Pdr1 with the
100 ergosterol biosynthetic pathway in this yeast. First, loss of *UPC2A* (*C. glabrata*
101 homologue of *C. albicans UPC2*) was sufficient to strongly reduce fluconazole
102 resistance of a GOF *PDR1* mutant allele (17). Second, genetic means of reducing the
103 flux through the ergosterol pathway led to induction of the Pdr pathway in a Upc2A-
104 dependent manner (18). Together, these data indicated that fluconazole resistance in
105 *C. glabrata* was likely to involve coordination of the Pdr1- and Upc2A-dependent
106 transcriptional circuits.
107 Given that Upc2A interfaced with the *PDR1* and *CDR1* promoters, we wanted to
108 determine the full spectrum of genes bound and regulated by this factor. This was
109 accomplished using chromatin immunoprecipitation coupled with Next Generation
110 Sequencing (ChIP-seq). We also performed RNA-seq studies to identify the Upc2A-
111 dependent transcriptome. Using the strong sequence conservation between *S.*
112 *cerevisiae* Upc2 and Upc2A, we constructed a GOF form of Upc2A in *C. glabrata* based
113 on an allele described for its *S. cerevisiae* homologue (19). This mutant Upc2A drove
114 elevated fluconazole resistance and behaved like the hyperactive *S. cerevisiae* factor.
115 ChIP-seq data indicated Upc2A bound to roughly 1000 genes and that this binding was

highly induced by fluconazole. Comparison of the genes bound by Upc2A with those we previously found to be associated with Pdr1 indicated a high degree of overlap between these two target gene suites. Upc2A-mediated transcription of *PDR1* and *CDR1* was linked with the response to anaerobic growth. Transcription of the *FKS1* gene, encoding a β-glucan synthase protein was also found to be responsive to Upc2A, consistent with *upc2AΔ* strains being hypersensitive to caspofungin which is thought to act as a β-glucan synthase inhibitor (reviewed in (20)). Our data provide a new view of the global importance of Upc2A-mediated transcriptional activation as extending far beyond its well-appreciated control of *ERG* gene expression. Upc2A appears to serve as a key coordinator of the biosynthesis of membrane lipids and proteins that are destined to function in this membrane environment.

Results

A gain-of-function form of Upc2A confers elevated fluconazole resistance.

Fluconazole resistance is most commonly caused in *C. glabrata* by substitution mutations within the *PDR1* gene (See (6, 21) for a review). These mutant transcription factors exhibit enhanced target gene expression when compared to the wild-type allele. Although mutations in the *UPC2* gene in both *Saccharomyces cerevisiae* and *Candida albicans* have been isolated that drive fluconazole resistance (22-24), there are no gain-of-function (GOF) forms currently known for *UPC2A*. To determine if a GOF allele of *UPC2A* could be produced, we constructed an allele based on analogy with a mutation first found in *Saccharomyces cerevisiae UPC2* (ScUpc2) which caused the enhanced

function of this transcriptional regulator (25). The relevant mutation (*upc2-1*) (19) is a change of a glycine to an aspartate residue located at position (G888D) in the carboxy-terminus of ScUpc2. Alignment of *C. glabrata* Upc2A and ScUpc2 indicated that G898 was the analogous position in Upc2A. This residue was replaced with an aspartate to form the G898D *UPC2A* form of the gene. The resulting mutant allele was tagged with a 3X hemagglutinin (3X HA) epitope at its amino terminus as we have previously done for the wild-type *UPC2A* gene and both these forms of *UPC2A* were integrated into an otherwise wild-type *C. glabrata* strain. These tagged strains were then grown to mid-log phase along with isogenic wild-type and *upc2A*Δ cells. Serial dilutions of each culture were placed on rich medium containing the indicated concentrations of fluconazole (Figure 1A).

Introduction of the G898D mutation into *UPC2A* led to the resulting factor exhibiting elevated fluconazole resistance when compared to either the tagged or untagged version of the wild-type gene. Loss of *UPC2A* caused a dramatic increase in fluconazole susceptibility. This is consistent with G898D *UPC2A* behaving as a hyperactive transcriptional activator in *C. glabrata* as has previously been seen for G888D Upc2 in *S. cerevisiae* (25).

To characterize the action of G898D Upc2A in control of fluconazole resistance, the expression of a range of different genes involved in this phenotype was examined by RT-qPCR. Our previous experiments have identified Upc2A as an inducer of expression of both the ATP-binding cassette transporter-encoding gene *CDR1* and the *PDR1* gene encoding a key transcriptional activator of *CDR1* (26). Levels of mRNA for

the *ERG11* gene, encoding the enzymatic target of fluconazole, as well as for *UPC2A* itself were also evaluated in the presence and absence of azole drug challenge.

The presence of the G898D *UPC2A* gene led to a strong elevation of *ERG11* transcription in the absence of fluconazole but had no significant effect on the other genes (Figure 1B). Treatment with fluconazole elevated transcription of all Upc2A target genes although the elevated *ERG11* mRNA levels seen in the absence of drug were not further induced by fluconazole when G898D Upc2A was present. The fluconazole induction of both *PDR1* and *CDR1* was enhanced by the presence of wild-type *UPC2A* relative to the presence of the GOF allele. *UPC2A* transcription was approximately two-fold elevated by fluconazole, irrespective of the *UPC2A* allele tested.

These same strains were then used to compare expression of their protein products by western analysis with appropriate antibodies. All strains were grown in the absence or presence of fluconazole and whole cell protein extracts prepared. These were analyzed by western blotting using the indicated antibodies (Figure 1C and D).

The presence of the G899D *UPC2A* allele supported normal fluconazole induction of Cdr1 and showed a modest reduction in Pdr1 activation. The levels of the wild-type and G898D forms of Upc2A were not detectably different as shown by blotting with the anti-Upc2A polyclonal antiserum. Over the time course of fluconazole challenge (two hours), no differences in the levels of these two forms of Upc2A were seen. These data argue that the increased activation seen for *ERG11* in the presence of the G898D *UPC2A* gene was due to increased function of Upc2A rather than a change in its expression compared to the wild-type factor.

Global analysis of Upc2A transcriptional targets. Having confirmed that the HA-tagged form of both wild-type and G898D Upc2A behaved as expected, we used these forms of Upc2A to carry out chromatin immunoprecipitation coupled with Next Generation Sequencing (ChIP-seq) to identify and compare genes that are direct transcriptional targets of Upc2A. Additionally, we assessed the effect of fluconazole induction on the suite of genes bound by either the wild-type or mutant forms of Upc2A. We also compared the binding sites found for Upc2A with those previously mapped for Pdr1 in ρ^0 cells (27) to determine the degree of overlap between these two transcriptional circuits involved in fluconazole resistance. The strains used above were grown to mid-log phase under control or fluconazole-treated conditions and fixed chromatin prepared and fragmented. Chromatin was immunoprecipitated with anti-HA antibody, purified and analyzed by Illumina sequencing. Reads were mapped and peaks called by use of the MACS2 algorithm (28). We first analyzed the peaks seen in these 4 different conditions (wild-type +/- fluconazole, mutant G898D +/- fluconazole) by determining the overlap of bound genes between them (Figure 2A).

The Venn diagram shown illustrates the extent of overlap between each different ChIP-seq reaction. The largest number of bound genes was seen for the wild-type factor in the presence of fluconazole (>1000 promoters bound). Interestingly, there were 565 of these promoters that only be bound Upc2A in the presence of fluconazole while others were bound in multiple different conditions. The next largest group of bound promoters (309) were found to be bound under all 4 different conditions. The third largest class of promoters (85) were only bound by Upc2A under conditions we consider induced (wild-type + fluconazole and G898D Upc2A +/- fluconazole). GO term

enrichment analysis of these three different classes of promoters indicated that very different genes were associated with these patterns of Upc2A DNA-binding. The largest class of genes was enriched for components of the translation apparatus (Supplementary table 1A). The class of genes bound under all 4 different conditions was most predominantly enriched for proteins associated with the plasma membrane (Supplementary table 1B) while the inducible class of Upc2A-bound promoters showed the strongest enrichment for genes involved in fatty acid biosynthesis (Supplementary table 1C). While all these genes are Upc2A target loci, they exhibited unique patterns of association with this factor.

We used the software MEME-ChIP to search the peaks associated with binding of wild-type Upc2A in the presence of fluconazole for sequence motifs that were enriched in this collection of binding sites. We chose this condition as it represented the broadest collection of sterol response elements (SREs). We compared the MEME-ChIP output to known binding sites for Upc2 in *S. cerevisiae* (ScUpc2) (29) and refer to the binding elements for Upc2A in *C. glabrata* as SREs on the basis of their similarity to those previously described in *S. cerevisiae* (30). This analysis is shown in Figure 2B.

The AR1b/c elements show the variation that is tolerated by Upc2 in *S. cerevisiae*. These ScUpc2 SREs are most closely fit to the right-hand element of the Upc2A SRE predicted by MEME-ChIP. The central CGTA sequence is conserved between *C. glabrata* and *S. cerevisiae*, although the *C. glabrata* element has a nearby conserved element (CACAGA) that shows a relatively constant spacing. It is important to note that all analyses of *S. cerevisiae* Upc2 DNA binding were carried out before the availability of global approaches like ChIP-seq which will impact predictions of

consensus elements as a more limited repertoire of regulated genes was considered. We examine the binding of Upc2A to its DNA target sites in detail below.

These data agree with the model proposed earlier that Upc2A appeared to accumulate inside the nucleus upon ergosterol limitation where the factor then binds to SRE-containing promoters (22). Since our previous work indicated overlap between Upc2A and Pdr1 target genes (26), we wanted to examine the degree of overlap between these different regulons. To make this comparison, we examined the shared Upc2A targets in cells treated with fluconazole (WTF) and the promoters bound by Pdr1 in ρ^0 cells (27). We selected these two conditions for comparison since both involve a signal that activates the wild-type versions of Upc2A and/or Pdr1 (fluconazole or loss of the mitochondrial genome, respectively) (8, 31). Strikingly, more than 50% of Pdr1 target promoters were also associated with Upc2A binding (Figure 2C). The top 4 GO terms enriched in genes bound by both these Zn_2Cys_6-containing transcription factors were associated with transmembrane transport or integral membrane components (Supplementary table 2). As our earlier work had shown that both *PDR1* and *CDR1* were targets of Upc2A along with Pdr1 (18), these new data indicate that the overlap between these two transcriptional circuits extends well beyond the initial two genes.

Two different classes of Upc2A target promoters are shown in Figure 2D. The *ERG11* gene is an example of a locus controlled by Upc2A but not Pdr1. Binding of wild-type Upc2A is represented by the read depth and can be seen to increase in the presence of fluconazole compared to in the absence of the drug. Binding of G898D Upc2A was constant, irrespective of the presence of the drug. Note that when the lack of a change in Upc2A expression is considered (see Figure 1C), these data support the

253 view that the DNA-binding activity of wild-type but not G898D Upc2A is increased by the
254 presence of fluconazole, possibly by an increase in nuclear localization (22).

255 *CDR1* represents a Upc2A target gene that is also regulated by Pdr1. The
256 bound regions for Pdr1 and Upc2A extensively overlap in the upstream region of *CDR1*.
257 Pdr1 DNA-binding was strongly upregulated in ρ^0 cells, likely due in part to the large
258 increase in *PDR1* expression in this background compared to wild-type cells (27).
259 Upc2A DNA-binding to *CDR1* was regulated in a manner similar to that seen for
260 *ERG11*.

261 The data above did not take into account a consideration of target gene
262 expression. In order to link regulated Upc2A binding to changes in gene transcription of
263 target genes, we carried out two additional analyses. First, we used software contained
264 within the MACS2 algorithm called BDGdiff (28) that examines ChIP-seq data and
265 identifies peaks that exhibit significant binding differences in the comparison of data
266 from fluconazole-treated cells versus untreated cells. Secondly, RNA-seq assays were
267 performed on isogenic wild-type and *upc2AΔ* cells in the presence and absence of
268 fluconazole. RNA-seq data were processed and we focused on genes that had an
269 adjusted P-value of <0.05 and significantly up-regulated by at least two-fold. These
270 data are summarized in Figure 3 and included in supplementary table 3.

271 Figure 3A represents the union of all genes that are induced in the presence of
272 fluconazole in either wild-type or *upc2AΔ* cells with genes that exhibited a significant
273 increase in Upc2A DNA-binding when comparing ChIP-seq data from cells grown in the
274 presence of fluconazole versus the absence of drug. Strikingly, only 53 genes required
275 the presence of Upc2A DNA-binding to be induced by fluconazole while 274 were

induced either in the presence or the absence of the *UPC2A* gene, although all these genes were bound by Upc2A. The majority of fluconazole-induced genes (542) were not dependent on the presence of Upc2A while 64 genes were fluconazole-induced, required the presence of Upc2A but were not bound by this factor.

These data argue that the vast number of fluconazole-induced genes do not depend on the presence of Upc2A. However, there are 117 genes that are only FLC-inducible in the presence of Upc2A. The only GO term enriched in the 64 genes that require the presence of Upc2A for FLC induction (yet are not bound by Upc2A) represent loci involved in ergosterol biosynthesis. These Upc2A-dependent but indirect targets include *ERG4*, *ERG8*, *ERG9*, *ERG24*, *ERG26* and *ERG27*. *ERG8* is in the earlier part of the ergosterol biosynthetic pathway while all other enzymes participate in the conversion of farnesyl pyrophosphate to ergosterol (recently reviewed in (32)).

The simplest class of fluconazole-induced genes are represented by the 53 direct target genes. GO terms enriched in this set of genes included ergosterol biosynthesis, plasma membrane and cell wall biogenesis, membrane transport, sterol uptake and RNA polymerase II core promoter-binding factors. The genes in this class of enriched genes include *UPC2B* and homologues of *S. cerevisiae NRG2* and *ADR1*. These factors may be involved in regulation of genes that are controlled indirectly by Upc2A.

The other two categories of fluconazole-regulated Upc2A-bound genes were either induced in both wild-type and *upc2A*Δ cells (201 genes) or only in the absence of *UPC2A* (73 genes). Only the group of 201 genes showed any significant GO term enrichment with specific groups of genes involved in the response to stress and glycogen catabolism being the top two categories.

The final and largest class of genes found to be bound by Upc2A were less than two-fold induced by fluconazole. GO term analysis of this class of genes indicated that the top three enriched categories were involved in translation and the ribosome (60 total). The next highest categories were plasma membrane or amino acid transmembrane transport and represented 74 genes. Together, these data strongly suggest that Upc2A impacts a wide range of cellular process as well as its well-described control of expression of genes involved in the ergosterol biosynthetic pathway.

To examine the range of expression of Upc2A-responsive genes, we compared the transcriptional response of a range of genes from the *ERG* pathway with loci that we have previously found to be targets of Pdr1 in *C. glabrata* (27). This comparison is presented in the form of a heat map (Figure 3B).

The majority of *ERG* genes showed at least two-fold induction by fluconazole in wild-type cells as long as these genes corresponded to steps later in the ergosterol biosynthetic pathway. *ERG10*, *ERG13*, *HMG1* and *ERG20*, which all encode early steps in ergosterol biosynthesis, were not influenced by fluconazole challenge in wild-type cells although expression of these genes was strongly depressed under these same conditions in the absence of *UPC2A*. Genes encoding enzymes that function later in ergosterol biosynthesis (like *ERG11*) were induced by fluconazole at least two-fold in wild-type cells but depressed by at least two-fold in a *upc2A*Δ background.

There were two *ERG* genes that were exceptions to these general trends of regulation. *ERG1*, one of the genes showing the best induction by fluconazole in wild-type cells and most prominent peak of Upc2A ChIP-seq density, was similarly drug

induced in both wild-type and *upc2AΔ* cells. *ERG8*, encoding an enzyme that functions early in the ergosterol pathway, was also similarly fluconazole-induced in both gene backgrounds, irrespective of the presence of Upc2A. Strikingly, *ERG8* was not seen to contain a detectable ChIP-seq peak for Upc2A binding. We interpret these complex responses to fluconazole treatment in *C. glabrata* as evidence for a multifactorial transcriptional network regulating *ERG* gene expression in which Upc2A participates as both a direct (later pathway genes) and indirect (early pathway genes) regulator.

Pdr1-regulated genes that were also associated with SREs exhibited less dependence on the presence of Upc2A for fluconazole induction than seen for most *ERG* genes. *CDR1* fluconazole induction was reduced upon loss of Upc2A but *PDR1* was similarly induced irrespective of the *UPC2A* background (Figure 3B). *SNQ2* and *PDH1* were reduced to approximately 50% of their normal drug-induced levels in the *upc2AΔ* strain while *QDR2* and *RTA1* showed higher levels of fluconazole induction in the same strain. Two other Pdr1 target genes (*PDR16*, *RSB1*) were repressed by the presence of fluconazole in wild-type cells and their expression lowered further when *upc2AΔ* cells were treated with fluconazole.

We also used RNA-seq to compare the gene expression profile of wild-type cells to an isogenic G898D *UPC2A* strain. These strains were grown to mid-log phase in the absence of fluconazole and then standard RNA-seq was carried out to determine the effects of this form of Upc2A on the transcriptome (Table 2).

The presence of the GOF form of *UPC2A* caused relatively small changes in gene transcription. There were only 11 genes observed to be elevated at least 1.4-fold. A striking feature shared by these genes was that nine of eleven encoded products that

were involved in the biosynthesis of ergosterol. Five of these 9 genes also contained SREs. As we have seen for *ERG11* (Figure 1B and C), the presence of the G898D Upc2A protein led to enhanced expression of multiple genes involved in ergosterol biosynthesis. This coordinate up-regulation is likely responsible for the observed increase in fluconazole resistance caused by this allele.

Identification of functional SREs in Upc2A target genes. To confirm that the SREs present in the direct Upc2A target genes were required for normal in vivo functions, we both mapped the location of several SREs and prepared mutant versions of these sites that could not normally interact with Upc2A. DNase I protection assays with a recombinant form of the Upc2A DNA-binding domain were used to locate each SRE at nucleotide resolution. Radioactive probes were prepared from SREs contained in the *ERG1*, *CDR1* and *PDR1* promoters. These probes were used in a DNase I protection mapping experiment to locate the bounds of the region protected by Upc2A from nuclease digestion. The DNase I ladders were electrophoresed in parallel with chemical sequencing reactions on the same probe in order to locate the SRE. These data are shown in Figure 4.

The *ERG1* promoter, which contains an everted pair of SREs (Figure 4A), showed the largest protected region of DNA and a strong DNase I hypersensitive site located immediately upstream of the SRE (Figure 4B). The *CDR1* SRE exhibited two DNase I hypersensitive sites linked to Upc2A binding while the *PDR1* SRE showed a clear protected region but no associated hypersensitive site.

Now that we could localize the SREs in each of these promoters to a relatively small segment of DNA, we mutagenized each to confirm its requirement for in vitro binding. To confirm that the predicted SREs were key for Upc2A binding, we used an electrophoretic mobility shift assay (EMSA) and prepared wild-type and mutant probes containing each SRE. Each probe was incubated with Upc2A and then resolved using nondenaturing electrophoresis. Bound and unbound probe was detected using a biotin moiety attached to the end of each probe. The results of this assay are shown in Figure 4C.

The wild-type *ERG1* probe produced two different species of protein:DNA complex, possibly corresponding to either one or two binding sites being occupied with Upc2A. The mutant form of this SRE blocked formation of both complexes. *CDR1* and *PDR1* probes both formed primarily a single size of complex that was greatly diminished when the mutant SRE probe was used. These data argue that the SREs indicated in Figure 4A are likely required for Upc2A binding to each promoter.

Phenotypes caused by loss of SRE function. To validate the importance of the SREs identified in *ERG1*, *CDR1* and *PDR1*, we prepared versions of these promoters that contained the mutations shown to block in vitro binding of Upc2A. These DNA-binding defective SREs (mSRE) were first introduced, along with their wild-type promoter, into a *lacZ* fusion plasmid to allow comparison of the expression supported by wild-type promoters to those that lacking Upc2A binding. These plasmids were transformed into wild-type cells, then grown to mid-log phase and challenged with or

without fluconazole. *C. glabrata* promoter-dependent β-galactosidase activity was then determined.

Introduction of the mSRE into *ERG1*, *CDR1* or *PDR1* promoters led to a reduction in the level of fluconazole-induced β-galactosidase activity produced by each respective fusion gene (Figure 5A). While some degree of fluconazole inducibility was retained in each mSRE-containing promoter, these data indicate that each SRE identified above is required for normal drug induced promoter activation.

To examine the effect of the loss of the SRE from the wild-type *CDR1* and *PDR1* genes, the mSRE mutations were introduced into otherwise wild-type versions of these two genes. Isogenic wild-type and mSRE versions of the *PDR1* locus were prepared by recombination into the normal chromosomal location of this gene in a strain containing a null allele of *CDR1*. Low-copy-number plasmids containing *CDR1* were constructed that varied only by the form of the SRE that was contained in the promoter region. These two different forms of *CDR1* were introduced into the wild-type and mSRE *PDR1* *cdr1Δ* strain and transformants grown in the presence or absence of fluconazole. Whole cell protein extracts were prepared and examined for expression of proteins of interest using appropriate polyclonal antisera (Figure 5B).

Loss of the SRE from the *CDR1* promoter caused a significant drop in expression when cells were treated with fluconazole that was enhanced when combined with the mSRE version of the *PDR1* gene. Similar reductions in Cdr1 levels were seen in the absence of fluconazole, again with removal of the SRE from both *CDR1* and *PDR1* causing the largest reduction in Cdr1 levels. Expression of Pdr1 was not affected when the *CDR1* SRE was removed but fluconazole induction of Pdr1 was reduced when the

412 SRE was removed from the *PDR1* promoter. Expression of Erg11 was unaffected in
413 these backgrounds as these alterations were restricted to the *CDR1* and *PDR1*
414 promoters.

415 These strains were also evaluated for their drug resistance phenotype using a
416 serial dilution assay on fluconazole-containing media (Figure 5C). The major reduction
417 in fluconazole resistance was caused by the presence of the mSRE-containing form of
418 the *CDR1* gene. This was modestly enhanced by the simultaneous loss of the SRE
419 from the *PDR1* gene. Together, these data demonstrate that the SREs present in
420 *CDR1* and *PDR1* are required for normal expression of these genes and for full
421 fluconazole resistance.

422

423 **Potential role for Pdr1/*CDR1* in anaerobic growth.** The above data continue to
424 support the notion that the Pdr pathway in *C. glabrata* is linked to levels of ergosterol as
425 we have argued previously (18). We wondered if a physiological parameter, key for
426 ergosterol biosynthesis, might also involve the Pdr pathway. To test this possibility, we
427 examined the effect of anaerobic growth on *PDR1* and *CDR1* expression. Oxygen is
428 essential for normal ergosterol biosynthesis and anaerobic growth triggers rapid
429 induction of *ERG* gene expression in several fungi, including *C. glabrata* (33). We also
430 evaluated the requirement for the presence of *PDR1* and *CDR1* during anaerobic
431 growth to test their contribution to this phenotype.

432 We validated our conditions of anaerobic growth by measuring the expression of
433 several genes known from work in *S. cerevisiae* to be induced under these conditions,
434 along with others that were repressed in the absence of oxygen (34). Wild-type cells

435 were grown aerobically or anaerobically, total RNA prepared and levels of mRNAs
436 assessed by RT-qPCR analyses.

437 Anaerobic growth led to 20-fold or higher induction of the genes corresponding to
438 products important in sterol uptake such as the ABC transporter Aus1 and other
439 proteins thought to be essential for this process (Dan1, Tir1) (Figure 6A). Anaerobic
440 growth also repressed expression of genes encoding mitochondrial proteins involved in
441 ATPase production (Atp3, Atp4) and an electron transport chain component (Sdh2).
442 Two different loci encoding enzyme involved in the tricarboxylic acid cycle were slightly
443 reduced (*KGD2*) or unaffected (*ACO1*).

444 Having confirmed that the expected anaerobic gene regulation was seen under
445 our growth conditions, we next tested expression of Cdr1, Pdr1 and Erg11 using the
446 western blot assay described previously (Figure 6B). Both Cdr1 and Pdr1 were strongly
447 induced, from 3- to 5-fold, while Erg11 was also induced albeit roughly 2-fold.

448 Since all these Upc2A target genes were induced in this assay, we wanted to
449 determine if the SREs associated with *CDR1* and *PDR1* were required for this
450 anaerobic activation. We used the strains described early in which either wild-type
451 versions of *CDR1* and *PDR1* were present or these same genes containing mutations in
452 their respective SREs were used. These isogenic strains were grown in the presence
453 or absence of oxygen and levels of Cdr1, Pdr1 and Erg11 (as a control for anaerobic
454 conditions) measured by western blotting.

455 Anaerobic induction of both Cdr1 and Pdr1 was diminished in the absence of the
456 SRE motifs in their promoters (Figure 6C). As seen before for fluconazole challenge,

457 the SREs in the *CDR1* and *PDR1* promoters are required for normal induction. Erg11
458 was not affected as its SRE was unaltered in this experiment.

459 To test if the expression of *CDR1* and *PDR1* was involved in normal anaerobic
460 growth, we carried out a competitive growth assay. Isogenic wild-type and double
461 mutant *cdr1Δ pdr1Δ* strains were mixed in equal portions and then grown under either
462 aerobic or anaerobic conditions. Once these mixed cultures had reached the end of log
463 phase growth, aliquots were plated to determine if the percentage of the populations
464 had changed.

465 The loss of *CDR1* and *PDR1* caused the resulting double mutant strain to exhibit
466 a growth disadvantage when competed with the wild-type parent (Figure 6D) but only
467 under anaerobic conditions. No change from the starting population was seen during
468 aerobic growth. These data provide evidence that Upc2A-regulated expression of both
469 *CDR1* and *PDR1* is required for normal anaerobic growth, linking the function of these
470 two genes to this phenotype for the first time.

471

472 **Role for Upc2A in caspofungin resistance**. The ChIP-seq data predicted a potential
473 SRE upstream of the *FKS1* and *FKS2* genes (Supplementary tables 1 and 2). To
474 determine if these putative SREs had detectable roles in expression of the caspofungin
475 resistance phenotype, we tested the ability of an isogenic set of strains varying in their
476 *UPC2A* allele for the response to several different cell wall stress agents. Isogenic wild-
477 type, *upc2AΔ* or epitope-tagged wild-type or G898D *UPC2A*-containing strains were
478 tested for resistance to caspofungin, caffeine or high pH using a serial dilution assay.
479 Caffeine and high pH are cell wall stresses and reflect general cell wall dysfunction (35).

Loss of *UPC2A* caused hypersensitivity to all these agents (Figure 7A) while both epitope-tagged alleles behaved like the wild-type strain. The finding of a caspofungin susceptible phenotype prompted us to examine expression of the three *FKS* genes in *C. glabrata* to determine if any of these showed a response to the G898D allele of *UPC2A*. None of these genes were altered in the presence of this gain-of-function form of *UPC2A* while both *ERG1* and *AUS1* were elevated (Figure 7B), confirming the functionality of this hypermorphic form of Upc2A.

To explain the observed caspofungin hypersensitivity of the *upc2AΔ* strain, levels of *FKS1* and *FKS2* mRNAs were measured using RT-qPCR in the presence or absence of caspofungin. Loss of *UPC2A* reduced basal expression of *FKS1* and had a modest effect on *FKS2* (Figure 7C). The addition of caspofungin strongly induced *FKS2* expression as expected (36) with this induction unaffected by the absence of Upc2A.

Since a defect was seen for *FKS1* expression, we prepared a DNA probe containing the putative SRE in this promoter for use in an EMSA to determine if recombinant Upc2A was able to recognize this element in vitro (Figure 7D). A mutant form of this SRE was also tested in this EMSA. The wild-type *FKS1* probe was strongly reduced in mobility when incubated with Upc2A while the mSRE-containing probe exhibited a band of reduced intensity upon loss of this sequence element.

To determine if the SRE was required for normal expression of *FKS1*, a *lacZ* translational fusion gene was prepared in which the *FKS1* regulatory region determined expression of β-galactosidase. Both the wild-type and mSRE-containing *FKS1* promoters were used and introduced on a low-copy-number plasmid into wild-type *C.*

502 *glabrata* cells. *FKS1*-dependent β-galactosidase activities were then determined in the
503 presence or absence of caspofungin induction.

504 Loss of the SRE from the *FKS1* promoter caused a significant reduction in *FKS1*-
505 dependent expression of *lacZ* in the absence of caspofungin (Figure 7E). These data
506 provide evidence that Upc2A-mediated gene activation is required for normal
507 expression of *FKS1* and wild-type caspofungin resistance.

508

509 Discussion

510 These data provide important new appreciation for the expansive role of Upc2A
511 in control of gene expression. Extensive previous work on Upc2A homologues in both
512 *S. cerevisiae* and *C. albicans* was generally done prior to the availability of modern
513 genomic approaches like ChIP- and RNA-seq (reviewed in (37)). Detailed analyses
514 demonstrated the crucial role of these Upc2A-like factors in regulation of *ERG* gene
515 biosynthesis (30, 38, 39)) but little was known about the full range of their target genes.
516 A ChIP-chip experiment was carried out on *C. albicans* Upc2 and this factor was found
517 to associate with the *CDR1* gene in this species (40). To the best of our knowledge,
518 there has been no follow-up linking *C. albicans* Upc2 with the Tac1 transcription factor
519 (key regulator of *CDR1* transcription) or *S. cerevisiae* Upc2 with either Sc*PDR1* or
520 Sc*PDR3*. This suggests the possibility that this *C. glabrata* connection between Upc2A
521 and Pdr1 is a unique feature of this yeast and could help explain the high level of
522 intrinsic azole resistance seen in this organism.

523 The large number of Upc2A target genes illustrates the breadth of processes that
524 are transcriptionally influenced by this factor. Clearly, the *ERG* genes are an important

set of genetic targets but these are a small fraction of the whole. Upc2A appears to be coordinating a broad group of genes including a large number of plasma membrane-localized proteins (See supplementary table 1 and 3). Coupled with its control of ergosterol in this membrane, Upc2A appears to be a central determinant of the composition of this membrane compartment in *C. glabrata*. The regulation of plasma membrane constituents is of obvious importance in modulating the ability of substances to cross this barrier between the external and internal environments.

Comparing the members of the target gene sets defined by Upc2A and Pdr1 suggests a hierarchical relationship between these two transcription factors. Here we establish that a binding site for Upc2A lies upstream of *PDR1* and is required for normal activation of *PDR1* expression (Figure 6C) as well as many of the other genes controlled directly by Pdr1. We suggest Upc2A provides overarching control of both the Pdr1 regulon but also a variety of other genes that are not under Pdr1 control, serving to link these different classes of genes through this common transcriptional regulation.

While the full range of Upc2A target genes illustrate the global importance of this transcription factor, the *ERG* genes are especially sensitive to the level of activity of this regulator. The G898D *UPC2A* allele has a surprisingly limited effect on gene expression as this allele was seen to trigger significant transcriptional changes almost exclusively in genes associated with ergosterol biosynthesis (Table 2). It is possible that the transcriptional impact of the G898D Upc2A could be expanded if cells were treated with fluconazole as ergosterol limitation might be able to impact expression by regulatory inputs beyond Upc2A. Experiments to test this possibility are underway.

Construction and analysis of G898D Upc2A demonstrated that there is no particular prohibition on hyperactive alleles of *UPC2A* existing in this pathogenic yeast. The *S. cerevisiae UPC2-1* allele, from we derived the G898D *UPC2A*, was originally isolated on the basis of permitting aerobic sterol uptake (19). Strikingly, no other *S. cerevisiae UPC2* hypermorphic alleles are known. *UPC2* mutations in *C. albicans* have been found in multiple clinical strains and appear to be much more commonly isolated (23, 24). An interesting feature of the majority of *C. albicans UPC2* GOF alleles is these all cluster with a region of the protein between residues 642 and 648 (16). This region shows strong sequence conservation with the 893-898 region of *C. glabrata* Upc2A. The conserved location of these hypermorphic alleles suggests the possibility that a common function is being disrupted in both organisms.

Based on detailed structural and subcellular localization studies on *S. cerevisiae* Upc2 (22), we propose that *C. glabrata* Upc2A accumulates in the nucleus upon ergosterol limitation. Our data support this assertion in two ways. First, a large increase in ChIP-seq peaks is seen for Upc2A when azole-treated cells are compared to untreated cells. Second, the G898D Upc2A mutant protein shows constitutively high number of ChIP-seq peaks that is not significantly altered by azole challenge. These data are consistent with a model in which Upc2A nuclear accumulation is enhanced upon ergosterol limitation and this regulation requires the function of the region containing G898 in the C-terminus of this factor.

The finding of the interaction between Upc2A and the *FKS1* gene provides an interesting connection between azole resistance, well-known to be impacted by Upc2A (41), and echinocandin resistance. These two antifungal drugs have been considered

570 to be defined by genetically separable pathways but here we provide evidence that
571 Upc2A may provide a link between them. Intervention in Upc2A-mediated
572 transcriptional activation may be able to cause reductions in resistance to both azole
573 drugs and the echinocandins.

574 Finally, our data also illuminate the complexity and interrelationship of expression
575 of genes involved in ergosterol biosynthesis with plasma membrane proteins and even
576 the cell wall. *ERG* gene regulation is an important task for Upc2A but this factor clearly
577 impacts transcription of a broad range of genes affecting multiple aspects of the plasma
578 membrane. Additionally, loss of Upc2A has clear phenotypes but is certainly not the
579 only regulator of *ERG* gene expression and fluconazole induction in *C. glabrata*. Loss
580 of *UPC2A* leads to a profound increase in fluconazole susceptibility, even in the
581 presence of a GOF form of *PDR1* (17). However, only ~50 genes were both bound by
582 Upc2A and dependent on Upc2A for fluconazole induction while 880 were induced in
583 the presence of fluconazole independent of Upc2A (Figure 3A). This provides an
584 illustration of the overlapping modes of regulation controlling gene expression in
585 response to ergosterol limitation. The importance of ergosterol production and its
586 synchronization with biogenesis of membrane proteins in the plasma membrane is
587 central to a fungal cell producing a normally functioning membrane that can allow
588 growth. Understanding this regulatory circuitry will allow interventions to be developed
589 that can restore and potentially even enhance azole susceptibility, allowing the use of
590 this highly effective antifungal drug to be maintained.
591
592

593 Materials and Methods

594

595 **Strains and growth conditions**. *C. glabrata* was routinely grown in rich YPD medium
596 [1% yeast extract, 2% peptone, 2% glucose] or under amino acid-selective conditions in
597 complete supplemental medium (CSM) (Difco yeast nitrogen extract without amino
598 acids, amino acid powder from Sunrise Science Products, 2% glucose). All solid media
599 contained 1.5% agar. Nourseothricin (Jena Bioscience, Jena, Germany) was
600 supplemented to YPD media at 50 µg/ml to select for strains containing the pBV133
601 vector (26) and its derivatives. All strains used in this study are listed in table 1.

602

603 **Plasmid construction and promoter mutagenesis.** All constructs used for
604 homologous recombination into the chromosome were constructed in a pUC19 plasmid
605 vector (New England Biolabs, Ipswich, MA). PCR was used to amplify DNA fragments
606 and Gibson assembly cloning (New England Biolabs) employed to assemble fragments
607 together. All isogenic deletion constructs were made by assembling the recyclable
608 cassette from pBV65 (26) and fragments from the immediate upstream/ downstream
609 regions of the target genes. Eviction of the recyclable cassette left a single copy of loxP
610 in place of the excised target gene coding region. Sequences of the repeated influenza
611 hemagglutinin epitope tag (3X HA) was PCR amplified from BVGC3 background (26).
612 This tag element was inserted before the start codon of *UPC2A* and G898D *UPC2A* with
613 an addition of repeated 3X glycine-alanine linker sequence located between the 3X HA
614 tag and the gene coding sequence. The G898D mutation in *UPC2A* was made by

615 Gibson assembly in which the overlapping primers contained the point mutation
616 sequence.
617
618 Gene complementation constructs were made by Gibson assembling the fragments
619 from the immediate upstream and downstream regions of the target genes [overlapping
620 regions], coding region of the target genes, target gene terminators (about 250 base-
621 pairs after the translation stop codon), and the recyclable cassette (located after the
622 terminator). Eviction of the recyclable cassette in the complementation constructs left a
623 single copy of loxP about 250 base-pairs downstream of the target gene stop codons.
624 Complementation of *LEU2* was done by PCR amplifying the *LEU2* coding region and
625 500 base-pairs immediate upstream and downstream of the coding region from the
626 CBS138 background. Linear DNA was then transformed into KKY2001 and the colonies
627 were selected on CSM agar without Leucine.
628
629 All autonomous plasmids were derived from pBV133 (26) carrying nourseothricin
630 marker. The *lacZ* gene encoding the *E. c*oli β-galactosidase gene was amplified from
631 pSK80 (42). *ERG1*, *CDR1*, *PDR1* promoter fragments were amplified from the
632 KKY2001 background. The *CDR1* minimal promoter, which was fused to *lacZ*,
633 contained the -1 to -1076 region (with the ATG of *CDR1* considered as +1). The full
634 *CDR1* promoter, which was used in the complementing plasmid, contained the -1 to -
635 1504 region. The *PDR1* promoter contained the -1 to -847 region in all constructs.
636 *ERG1* promoter region consisted of the -1 to -916 region and the *FKS1* promoter
637 contained the -1 to -1795 region. SRE mutations in the target gene promoters were

done by modifying the SRE core sequence and 2 adjacent bases into a PacI restriction enzyme sequence with Gibson assembly in which the overlapping primers contained the PacI sequence. All constructs were verified by Sanger sequencing (University of Iowa Genomic Core)

***C. glabrata* transformation.** Cell transformations were performed using a lithium acetate method (43). After being heat shocked, cells were either directly plated onto selective CSM agar plates (for auxotrophic complementation) or grown at 30°C at 200 rpm overnight (for nourseothricin selection). Overnight cultures were then plated on YPD or CSM agar plates supplemented with 50 µg/ml of nourseothricin. Plates were incubated at 30°C for 24 to 48 h before individual colonies were isolated and screened by PCR for correct insertion of the targeted construct.

Expression and purification of Upc2A DNA binding domain. The DNA sequence corresponding to the first 150 amino acids of the N-terminus of Upc2A was amplified by PCR and cloned into pET28a+ vector [digested with NcoI and SacI] with Gibson cloning. Correct clones were sequenced verified and transformed into the BL21 DE3 *E. coli* expression strain (Thermo Fisher, Waltham, MA). Mid-log phase cells were induced with 1 mM IPTG (Fisher Scientific, Hampton, NH) for 4 hours at 30ºC. Collected cells were lysed using a French Press G-M high pressure disruptor (GlenMills, Clifton, NJ). The clarified lysate was subjected to Talon Metal Affinity column (Takara, Mountain View, CA) as per the manufacturer's protocol**.** Purified protein was dialyzed with dialysis buffer

660 [20 mM Tris pH 8.0, 500 mM NaCl, 1 mM dithiothreitol and 0.5% Tween 20] for 24 hours
661 and its concentration was quantified by Bradford assay (Bio-Rad, Des Plaines, IL).
662
663 **Quantification of transcript levels by RT-qPCR.** Total RNA was extracted from cells
664 by extraction using TRIzol (Invitrogen, Carlsbad, CA) and chloroform (Fisher Scientific,
665 Hampton, NH) followed by purification with RNeasy minicolumns (Qiagen, Redwood
666 City, CA). RNA was reverse-transcribed using an iScript cDNA synthesis kit (Bio-Rad,
667 Des Plaines, IL). Assay of RNA via quantitative PCR [qPCR] was performed with iTaq
668 universal SYBR green supermix (Bio-Rad). Target gene transcript levels were
669 normalized to transcript levels of 18S rRNA during fluconazole challenge and β-tubulin
670 mRNA in other conditions. Primer sequences were listed in supplementary table 4.
671
672 **Spot test assay.** Cells were grown in YPD medium to mid-log-phase. Cultures were
673 then 10-fold serially diluted and spotted onto YPD agar plates containing different
674 concentrations [10 or 20 μg/ml] of fluconazole (LKT laboratories, St Paul, MN),
675 caspofungin 100 ng/ml (Apexbio, Houston, TX), congo red 100 μg/ml (Sigma-Aldrich,
676 St. Louis, MO), caffeine (Sigma-Aldrich). In some experiments, the YPD medium and
677 agar was supplemented with 50 μg/ml nourseothricin to maintain plasmids derived from
678 the pBV133 vector (26). All agar plates were incubated at 30°C for 24 to 48 h before
679 imaging was performed. To adjust the pH level, 100 mM of MES (VWR, Radnor, PA)
680 [pH 5.5], HEPES (RPI) [pH 7.0], and TAPS (Sigma-Aldrich) [pH 8.0] were added to the
681 2x YPD. Solutions were then filtered and mixed with autoclaved 3% agar to make YPD
682 agar plates.

683

684 **Competitive growth assay.** The *LEU2* coding region along with its immediate 500 bps
685 upstream and downstream sequences were amplified from CBS138 genomic DNA. The
686 product was then used to restore *LEU2* in mSRE *PDR1*/mSRE *CDR1* [KKY2001
687 background] and *pdr1*Δ/*cdr1*Δ at its native locus to generate mSRE *PDR1*/mSRE
688 *CDR1*/*LEU2* and *pdr1*Δ/*cdr1*Δ/*LEU2*. In the fluconazole competitive growth assay, mid-
689 log growth culture [between OD of 1 and 2] was diluted to 0.5 O.D. in fresh YPD. 1:1
690 ratio of *PDR1 CDR1* and mSRE *PDR1*/mSRE *CDR1* cultures were mixed together, and
691 treated either with fluconazole [20 µg/ml] or ethanol. At each time point, culture was
692 collected, serially diluted, and plated on YPD and synthetic complete media without
693 leucine for CFU determination.

694

695 In the anaerobic growth competitive assay, KKY2001 and its isogenic *pdr1*Δ *cdr1*Δ
696 derivative were diluted to 0.01 O.D. and the mixed culture [1:1 ratio] was grown either
697 aerobically [normoxic] or anaerobically [in a GasPak chamber (BD Biosciences, San
698 Jose, CA)] for 24 hours. 1 mM Acetyl CoA (Sigma-Aldrich), 1% Tween80/Ethanol [1:1
699 ratio], 1 mM Squalene (VWR), 50 µM Lanosterol (Sigma-Aldrich), 50 µM Ergosterol
700 (Sigma-Aldrich) were added to the mixed culture before the incubation. Acetyl CoA
701 stock solution was made in sterile H_2O, and all sterol stock solutions were made in
702 Tween80/Ethanol (1:1 ratio).

703

704 **Electrophoretic mobility shift assays (EMSA).** DNA probes were amplified by PCR
705 with biotinylated primers (IDT, Coralville, IA) corresponding to the sequences listed in

706 S2 table. Fragments from the *ERG1* promoter -704 to -916, *CDR1* promoter -560 to -
707 731, *PDR1* promoter -552 to -728, *FKS1* promoter -1489 to-1666, and *HO* promoter -
708 787 to-957 regions were amplified. Reaction buffer [18 µl], containing 5 µg sheared
709 salmon sperm DNA (Thermo Fisher Scientific, Waltham, MA), 5% Glycerol, 0.01%
710 NP40, 0.1% bovine serum albumin (Thermo Fisher Scientific), and 2 µl of 10x binding
711 buffer [100 mM Tris pH 7.5, 400 mM NaCl, 10 mM DTT and 100 µM $ZnSO_4$], was
712 incubated with different concentrations of Upc2A-6X His or 1X binding buffer for 10
713 minutes at room temperature. Biotinylated probes [20 fmol] were added in a final
714 reaction volume of 20 µl and incubated for additional 20 min at room temperature.
715 Samples were immediately subjected to electrophoresis on 5% polyacrylamide
716 Tris/Borate/EDTA [TBE] gel in 0.5x TBE running buffer at 4^{o}C. Subsequently, samples
717 were transferred into a nylon membrane (GE, Chicago, IL) in 0.5X TBE buffer at 4^{o}C.
718 Samples were then crosslinked on nylon membrane under UV light for 10 min.
719 Membrane was blocked with Intercept blocking buffer (LI-COR Biosciences, Lincoln,
720 NE) containing 1% SDS for 30 min before IRDye 680LT Streptavidin (LI-COR
721 Biosciences) antibody was added at 1:20000 final dilution. After 35 min of incubation,
722 the membrane was washed three times with phosphate buffer saline [PBS] containing
723 0.1% tween (RPI). Imaging was performed with Odyssey CLx Imaging System (LI-COR
724 Biosciences) and analyzed by Image Studio Lite Software (LI-COR Biosciences).
725
726 **Chromatin immunoprecipitation-Next Generation Sequencing.** Overnight cultures
727 were inoculated at 0.1 OD/ml in fresh YPD and allowed to grow to 0.4-0.5 OD/ml. Cells
728 were treated with Fluconazole 20 µg/ml or ethanol for 2 hours. Cells were fixed with 1%

729 formaldehyde (Sigma-Aldrich) for 15 min at room temperature with mild shaking [120-
730 150 rpm]. The fixing reaction was stopped with 250 mM glycine (RPI) for 15 min at room
731 temperature with mild shaking [120-150 rpm]. Cells were centrifuged and washed once
732 with PBS. The cell pellet was resuspended in lysis buffer [50mM Hepes pH 7.5, 140mM
733 NaCl, 1mM EDTA, 1% Triton X-100, 0.1% Sodium deoxycholate, 1mM PMSF, 1x
734 protease inhibitor cocktail (Roche Applied Science, Penzberg, Germany). Cells were
735 then lysed with 1 ml glass beads (Scientific Industries Inc, Bohemia, NY) at 4^{o}C for 10
736 min. Both cell lysate and debris were collected and subsequently transferred to an AFA
737 fiber pre-slit snap-cap [6 x 15mm] microtube (Covaris, Woburn, MA) for additional
738 cellular lysis and DNA shearing.
739
740 Genomic DNA was sheared with E220 focused-ultrasonicator (Covaris) [peak incident
741 power: 75 W, duty factor: 10%, cycles per burst: 200, treatment time: 16 min,
742 temperature: 10^{o}C max, sample volume: 130 µl.] The sheared sample was centrifuged
743 and the clear lysate was collected. Upc2A was immunoprecipitated with Dyna beads-
744 protein G magnetic beads (Invitrogen, Carlsbad, CA) and anti-HA antibody (Invitrogen)
745 [1:50 dilution] overnight at 4^{o}C. Beads were then washed twice with lysis buffer, once
746 with lysis buffer+ 500mM NaCl, once with LiCl buffer [10 mM Tris pH 8, 250 mM LiCl,
747 0.5% P-40, 0.5% Sodiumdeoxycholate, and 1 mM EDTA], and once with Tris-EDTA
748 buffer. Beads were resuspended in TE and treated with RNAse A (Thermo Fisher
749 Scientific) at 37^{o}C for 30 min. Beads were then washed once with Tris-EDTA buffer,
750 resuspended in Tris-EDTA buffer with 1% SDS, and incubate at 65^{o}C for at least 5
751 hours to reverse crosslink. Eluted DNA was subsequently purified with mini elite clean-

752 up kit (Qiagen). Qubit fluorometric assay (Thermo Fisher Scientific) was used to analyze
753 the yield quantity and Agilent Bioanalyzer (Agilent Technology, Santa Clara, CA) was
754 used to determine the average sheared DNA size.
755
756 All ChIPed DNA libraries were generated with Accel-NGS plus DNA library kit (Swift
757 Biosciences, Ann Arbor, MI) according to the manufacturer's instructions. Samples
758 were sequenced at the University of Iowa Institute for Human Genetics Genomics
759 Division using an Illumina NovaSeq 6000 instrument. Read quality was confirmed using
760 FastQC (Babraham Bioinformatics). The reads from duplicate experiments were
761 combined and mapped to the *C. glabrata* CBS138 genome using HISAT2 (44). Paired
762 reads with intervening fragments greater than 1000 bp were removed during the
763 mapping. The total number of mapped reads were reduced by randomly selecting 2.5%
764 from each bam file which were then sorted and indexed using Samtools. ChiP-seq
765 peak calling was done with the callpeak function of MACS2 using a false discovery rate
766 (q-value) cutoff of 0.001 and a maximum allowable gap between peaks of 100 bp (28).
767 Differential peak detection among the experimental conditions was done using the
768 bdgdiff function of MACS2. The default likelihood ratio cutoff of 1000 was used. Output
769 files from both callpeak and bdgdiff were annotated to identify candidate downstream
770 genes using the ChIPpeakAnno R package (45).
771
772 **RNA-sequencing**. A single colony of each *C. glabrata* strain was used to inoculate 2
773 ml of YPD, which was grown overnight at 30° C in an environmental shaking incubator.
774 Cell density was then adjusted to OD_{600}=0.1 in 10 ml YPD, and cultures were grown as

before for 6 hrs (mid-log phase). For the fluconazole-treated strains, either fluconazole (50 μg/ml final concentration) or DMSO (diluent control) was added to the 10 ml culture and grown for 6 hrs. Cells were collected by centrifugation, supernatants discarded, and cell pellets stored at -80° C. RNA was isolated from cell pellets via a hot phenol method as described previously (46) . The quantity and purity of RNA were determined by spectrophotometer (NanoDrop Technologies, Inc., Wilmington, DE) and verified using a Bioanalyzer 2100 (Agilent Technologies, Santa Clara, CA). Library preparation and RNA sequencing analysis were performed as previously described (47). Transcript quantification of expression levels and analysis of differential expression were done using HISAT2 and Stringtie (48). Differential expression was analyzed using DESeq2 (49).

DNase I protection assay. DNA probes were generated by PCR. To generate a 5′ [γ-^{32}P] singly end-labelled probe one of the PCR primers was modified [5 Amino-MC6 (Integrated DNA technologies, Coralville,IA)] at the 5′ end to prevent phosphorylation by polynucleotide kinase. Probes were end-labelled [1 pmol] using 10 μCi of [γ-^{32}P]-ATP (PerkinElmer, Waltham, MA) and 10 U polynucleotide kinase (New England Biolabs, Beverly, MA) as instructed by the manufacturer. Unincorporated [γ-^{32}P]-ATP was removed using a nucleotide removal column (Qiagen). The binding reaction was done as described in the EMSA section, and the sample was digested with DNase I (NEB [1:20 dilution]) for 30 seconds at room temperature. DNase I foot-printing and DNA sequencing reactions were performed as previously described (50).

β-galactosidase assay. Harvested cells were lysed with glass beads (Scientific Industries Inc) in breaking buffer [100 mM Tris pH8, 1 mM Dithiothreitol, and 20% Glycerol] at 4°C for 10 min. Lysate was collected and β-galactosidase reactions carried out in Z-buffer [60 mM Na_2HPO_4, 40 mM NaH_2PO_4, 10 mM KCl, 1 mM $MgSO_4$, 50 mM 2-Mercaptoethanol] with 650 µg /ml O-nitrophenyl-β-D-galactoside [ONPG]. Miller units were calculated based on the equation: [OD_{420} x 1.7] / [0.0045 x total protein concentration x used extract volume x time]. The Bradford assay (Bio-Rad) was used to measure the total protein concentration in the lysate.

Western immunoblot. Cells were lysed with lysis buffer [1.85 M NaOH, 7.5% 2-Mercaptoethanol]. Proteins were precipitated with 50% Trichloroacetic acid and resuspended in Urea buffer [40 mM Tris pH8, 8.0 M Urea, 5% SDS, 1% 2-Mercaptoethanol]. Cdr1, Pdr1, and Upc2A rabbit polyclonal antibodies were previously described (18, 27). Mouse anti-HA monoclonal antibody was purchased from Invitrogen. Secondary antibodies were purchased from LI-COR Biosciences. Imaging was performed with Odyssey CLx Imaging System (LI-COR Biosciences) and analyzed by Image Studio Lite Software (LI-COR Biosciences). Detected target band fluorescence intensity was normalized against tubulin fluorescence intensity and compiled from 2 biological replicate experiments and 2 technical replicates in each experiment, giving 4 replicates in total.

Statistical analysis. Unpaired T-test was used to compare between isogenic deletion mutant and wildtype strains. Paired T-test was used to compare between the drug

821 treated and non-treated conditions. *, **, *** were designated for P ≦ 0.05, 0.01, 0.001
822 respectively.
823
824 Acknowledgements
825 We thank Dr. Damian Krysan for helpful discussions.
826
827 References

828 1. Denning DW, Bromley MJ. Infectious Disease. How to bolster the antifungal
829 pipeline. Science. 2015;347(6229):1414-6.
830 2. Arastehfar A, Gabaldon T, Garcia-Rubio R, Jenks JD, Hoenigl M, Salzer HJF, et
831 al. Drug-Resistant Fungi: An Emerging Challenge Threatening Our Limited Antifungal
832 Armamentarium. Antibiotics (Basel). 2020;9(12).
833 3. Lass-Florl C. Triazole antifungal agents in invasive fungal infections: a
834 comparative review. Drugs. 2011;71(18):2405-19.
835 4. Perfect JR, Ghannoum M. Emerging Issues in Antifungal Resistance. Infect Dis
836 Clin North Am. 2020;34(4):921-43.
837 5. Pfaller MA, Diekema DJ, Turnidge JD, Castanheira M, Jones RN. Twenty Years
838 of the SENTRY Antifungal Surveillance Program: Results for Candida Species From
839 1997-2016. Open Forum Infect Dis. 2019;6(Suppl 1):S79-S94.
840 6. Arendrup MC, Patterson TF. Multidrug-Resistant Candida: Epidemiology,
841 Molecular Mechanisms, and Treatment. J Infect Dis. 2017;216(suppl_3):S445-S51.
842 7. Vermitsky JP, Edlind TD. Azole resistance in Candida glabrata: coordinate
843 upregulation of multidrug transporters and evidence for a Pdr1-like transcription factor.
844 Antimicrob Agents Chemother. 2004;48(10):3773-81.
845 8. Tsai HF, Krol AA, Sarti KE, Bennett JE. Candida glabrata PDR1, a transcriptional
846 regulator of a pleiotropic drug resistance network, mediates azole resistance in clinical
847 isolates and petite mutants. Antimicrob Agents Chemother. 2006;50(4):1384-92.
848 9. Whaley SG, Rogers PD. Azole Resistance in Candida glabrata. Current
849 infectious disease reports. 2016;18(12):41.
850 10. Sanglard D, Ischer F, Calabrese D, Majcherczyk PA, Bille J. The ATP binding
851 cassette transporter gene CgCDR1 from Candida glabrata is involved in the resistance
852 of clinical isolates to azole antifungal agents. Antimicrob Agents Chemother.
853 1999;43(11):2753-65.
854 11. Paul S, Moye-Rowley WS. Multidrug resistance in fungi: regulation of transporter-
855 encoding gene expression. Frontiers in physiology. 2014;5:143.
856 12. Siopi M, Tarpatzi A, Kalogeropoulou E, Damianidou S, Vasilakopoulou A, Vourli
857 S, et al. Epidemiological Trends of Fungemia in Greece with a Focus on Candidemia
858 during the Recent Financial Crisis: a 10-Year Survey in a Tertiary Care Academic
859 Hospital and Review of Literature. Antimicrob Agents Chemother. 2020;64(3).

13. Coste AT, Karababa M, Ischer F, Bille J, Sanglard D. TAC1, transcriptional activator of CDR genes, is a new transcription factor involved in the regulation of Candida albicans ABC transporters CDR1 and CDR2. Eukaryot Cell. 2004;3(6):1639-52.
14. Morschhauser J, Barker KS, Liu TT, Blab-Warmuth J, Homayouni R, Rogers PD. The transcription factor Mrr1p controls expression of the MDR1 efflux pump and mediates multidrug resistance in Candida albicans. PLoS Pathog. 2007;3:e164.
15. Perea S, Lopez-Ribot JL, Kirkpatrick WR, McAtee RK, Santillan RA, Martinez M, et al. Prevalence of molecular mechanisms of resistance to azole antifungal agents in Candida albicans strains displaying high-level fluconazole resistance isolated from human immunodeficiency virus-infected patients. Antimicrob Agents Chemother. 2001;45(10):2676-84.
16. Flowers SA, Barker KS, Berkow EL, Toner G, Chadwick SG, Gygax SE, et al. Gain-of-function mutations in UPC2 are a frequent cause of ERG11 upregulation in azole-resistant clinical isolates of Candida albicans. Eukaryot Cell. 2012;11(10):1289-99.
17. Whaley SG, Caudle KE, Vermitsky JP, Chadwick SG, Toner G, Barker KS, et al. UPC2A is required for high-level azole antifungal resistance in Candida glabrata. Antimicrob Agents Chemother. 2014;58(8):4543-54.
18. Vu BG, Thomas GH, Moye-Rowley WS. Evidence that Ergosterol Biosynthesis Modulates Activity of the Pdr1 Transcription Factor in Candida glabrata. MBio. 2019;10(3).
19. Crowley JH, Leak FW, Jr., Shianna KV, Tove S, Parks LW. A mutation in a purported regulatory gene affects control of sterol uptake in Saccharomyces cerevisiae. J Bacteriol. 1998;180(16):4177-83.
20. McCormack PL, Perry CM. Caspofungin: a review of its use in the treatment of fungal infections. Drugs. 2005;65(14):2049-68.
21. Healey KR, Perlin DS. Fungal Resistance to Echinocandins and the MDR Phenomenon in Candida glabrata. J Fungi (Basel). 2018;4(3).
22. Yang H, Tong J, Lee CW, Ha S, Eom SH, Im YJ. Structural mechanism of ergosterol regulation by fungal sterol transcription factor Upc2. Nat Commun. 2015;6:6129.
23. Heilmann CJ, Schneider S, Barker KS, Rogers PD, Morschhauser J. An A643T mutation in the transcription factor Upc2p causes constitutive ERG11 upregulation and increased fluconazole resistance in Candida albicans. Antimicrob Agents Chemother. 2010;54(1):353-9.
24. Hoot SJ, Smith AR, Brown RP, White TC. An A643V amino acid substitution in Upc2p contributes to azole resistance in well-characterized clinical isolates of Candida albicans. Antimicrob Agents Chemother. 2011;55(2):940-2.
25. Davies BS, Wang HS, Rine J. Dual activators of the sterol biosynthetic pathway of Saccharomyces cerevisiae: similar activation/regulatory domains but different response mechanisms. Mol Cell Biol. 2005;25(16):7375-85.
26. Vu BG, Moye-Rowley WS. Construction and Use of a Recyclable Marker To Examine the Role of Major Facilitator Superfamily Protein Members in Candida glabrata Drug Resistance Phenotypes. mSphere. 2018;3(2).

27. Paul S, Bair TB, Moye-Rowley WS. Identification of Genomic Binding Sites for Candida glabrata Pdr1 Transcription Factor in Wild-Type and rho0 Cells. Antimicrob Agents Chemother. 2014;58(11):6904-12.
28. Zhang Y, Liu T, Meyer CA, Eeckhoute J, Johnson DS, Bernstein BE, et al. Model-based analysis of ChIP-Seq (MACS). Genome Biol. 2008;9(9):R137.
29. Gallo-Ebert C, Donigan M, Stroke IL, Swanson RN, Manners MT, Francisco J, et al. Novel antifungal drug discovery based on targeting pathways regulating the fungus-conserved Upc2 transcription factor. Antimicrob Agents Chemother. 2014;58(1):258-66.
30. Vik A, Rine J. Upc2p and Ecm22p, dual regulators of sterol biosynthesis in Saccharomyces cerevisiae. Mol Cell Biol. 2001;21(19):6395-405.
31. Paul S, Schmidt JA, Moye-Rowley WS. Regulation of the CgPdr1 transcription factor from the pathogen Candida glabrata. Eukaryot Cell. 2011;10(2):187-97.
32. Jorda T, Puig S. Regulation of Ergosterol Biosynthesis in Saccharomyces cerevisiae. Genes (Basel). 2020;11(7).
33. Li QQ, Tsai HF, Mandal A, Walker BA, Noble JA, Fukuda Y, et al. Sterol uptake and sterol biosynthesis act coordinately to mediate antifungal resistance in Candida glabrata under azole and hypoxic stress. Mol Med Rep. 2018;17(5):6585-97.
34. Kwast KE, Lai LC, Menda N, James DT, 3rd, Aref S, Burke PV. Genomic analyses of anaerobically induced genes in Saccharomyces cerevisiae: functional roles of Rox1 and other factors in mediating the anoxic response. J Bacteriol. 2002;184(1):250-65.
35. Fuchs BB, Mylonakis E. Our paths might cross: the role of the fungal cell wall integrity pathway in stress response and cross talk with other stress response pathways. Eukaryot Cell. 2009;8(11):1616-25.
36. Katiyar SK, Alastruey-Izquierdo A, Healey KR, Johnson ME, Perlin DS, Edlind TD. Fks1 and Fks2 are functionally redundant but differentially regulated in Candida glabrata: implications for echinocandin resistance. Antimicrob Agents Chemother. 2012;56(12):6304-9.
37. Espenshade PJ, Hughes AL. Regulation of sterol synthesis in eukaryotes. Annu Rev Genet. 2007;41:401-27.
38. Silver PM, Oliver BG, White TC. Role of Candida albicans transcription factor Upc2p in drug resistance and sterol metabolism. Eukaryot Cell. 2004;3(6):1391-7.
39. MacPherson S, Akache B, Weber S, De Deken X, Raymond M, Turcotte B. Candida albicans zinc cluster protein Upc2p confers resistance to antifungal drugs and is an activator of ergosterol biosynthetic genes. Antimicrob Agents Chemother. 2005;49(5):1745-52.
40. Znaidi S, Weber S, Al-Abdin OZ, Bomme P, Saidane S, Drouin s, et al. Genomewide location analysis of Candida albicans Upc2p, a regulator of sterol metabolism and azole drug resistance. Eukaryot Cell. 2008;7:836-47.
41. Nagi M, Nakayama H, Tanabe K, Bard M, Aoyama T, Okano M, et al. Transcription factors CgUPC2A and CgUPC2B regulate ergosterol biosynthetic genes in Candida glabrata. Genes Cells. 2011;16(1):80-9.
42. Khakhina S, Simonicova L, Moye-Rowley WS. Positive autoregulation and repression of transactivation are key regulatory features of the Candida glabrata Pdr1 transcription factor. Mol Microbiol. 2018;107(6):747-64.

950 43. Ito H, Fukuda Y, Murata K, Kimura A. Transformation of intact yeast cells treated
951 with alkali cations. J Bacteriol. 1983;153:163-8.
952 44. Kim D, Paggi JM, Park C, Bennett C, Salzberg SL. Graph-based genome
953 alignment and genotyping with HISAT2 and HISAT-genotype. Nat Biotechnol.
954 2019;37(8):907-15.
955 45. Zhu LJ, Gazin C, Lawson ND, Pages H, Lin SM, Lapointe DS, et al.
956 ChIPpeakAnno: a Bioconductor package to annotate ChIP-seq and ChIP-chip data.
957 BMC bioinformatics. 2010;11:237.
958 46. Schmitt ME, Brown TA, Trumpower BL. A simple and rapid method for
959 preparation of RNA from S. cerevisiae. Nucl Acids Res. 1990;18:3091-2.
960 47. Whaley SG, Caudle KE, Simonicova L, Zhang Q, Moye-Rowley WS, Rogers PD.
961 Jjj1 Is a Negative Regulator of Pdr1-Mediated Fluconazole Resistance in Candida
962 glabrata. mSphere. 2018;3(1).
963 48. Pertea M, Kim D, Pertea GM, Leek JT, Salzberg SL. Transcript-level expression
964 analysis of RNA-seq experiments with HISAT, StringTie and Ballgown. Nat Protoc.
965 2016;11(9):1650-67.
966 49. Love MI, Huber W, Anders S. Moderated estimation of fold change and
967 dispersion for RNA-seq data with DESeq2. Genome Biol. 2014;15(12):550.
968 50. Paul S, Stamnes M, Thomas GH, Liu H, Hagiwara D, Gomi K, et al. AtrR Is an
969 Essential Determinant of Azole Resistance in Aspergillus fumigatus. MBio. 2019;10(2).
970

971 Figure Legends

972

973 Figure 1. **Characterization of *UPC2A* gain-of-function allele.** A. An isogenic series
974 of strains was prepared that varied in their *UPC2A* allele: wild-type (CBS138), *upc2A*Δ,
975 or strains containing an amino-terminally HA-tagged form of wild-type (3X HA-*UPC2A*)
976 or the G898D form of *UPC2A* (3X HA-G898D *UPC2A*). These strains were grown to
977 mid-log phase and then tested for their resistance to the indicated levels of fluconazole
978 in rich medium. B. G898D Upc2A induced *ERG11* mRNA under basal conditions. The
979 strains described in A were grown in the presence or absence of fluconazole and total
980 RNA prepared. Levels of mRNA were assessed by RT-qPCR. C. Western blot
981 analysis of Upc2A and target gene-encoded proteins. The indicated strains were grown
982 as described previously in the presence or absence of fluconazole, whole cell protein

983 extracts prepared and analyzed by western blotting using the antisera listed at the left
984 side. Upc2A was detected using either an anti-Upc2A polyclonal antibody (α-Upc2A) or
985 anti-HA (α-HA). Tubulin was used as a loading control along with Ponceau S staining of
986 the membranes. Quantitation shown in the right hand panel was performed as
987 described in Materials and Methods.
988
989 Figure 2. **Chromatin immunoprecipitation-high throughput sequencing (ChIP-seq)**
990 **analysis of *UPC2A*.** A. 3X HA-tagged forms of either the wild-type (WT) or G898D
991 (M)alleles of *UPC2A* were used for a standard ChIP-seq experiment. Strains were in
992 the presence (WTF, MF) or absence (WT, M) of fluconazole, followed by ChIP-seq
993 analysis as described earlier (27). A Venn diagram showing the overlap of genes
994 detected in each sample is shown with largest number of genes color-coded from dark
995 to light. B. MEME-ChIP analysis of sterol response element (SREs) shared in Upc2A
996 peaks. A logo is shown representing the most commonly enriched element associated
997 with Upc2A ChIP-seq peaks that was detected by MEME-ChIP analysis. AR1b and
998 AR1c show the corresponding Upc2 consensus sites from *Saccharomyces cerevisiae*
999 (29). C. Venn diagram showing the overlap between binding sites found for
1000 fluconazole-stressed 3X HA-*UPC2A* (WTF) and ρ^0-induced wild-type Pdr1 (27). D.
1001 Comparison of Upc2A- and Pdr1-binding to the *CDR1* and *ERG11* promoters. Plots of
1002 relative ChIP-seq density are shown for ChIP reactions performed with either anti-Pdr1
1003 or α-HA to detect epitope-tagged Upc2A. ChIP in samples treated with fluconazole is
1004 denoted +F while the corresponding no drug control is represented by -F. The bottom

line is a control ChIP reaction using wild-type cells that lack the HA-epitope tag (Upc2A). *CDR1* is controlled by both factors while *ERG11* only responds to Upc2A.

Figure 3. **RNA-seq analysis of fluconazole induced genes in wild-type and *upc2AΔ* strains.** A. Venn diagrams illustrating the union of genes that are at least two-fold induced in wild-type (2X Induced WTF) or isogenic *upc2AΔ* cells treated with fluconazole along with genes containing a Upc2A SRE that is exhibits fluconazole inducible binding compared to untreated samples (WTF over WT). B. Heat map of representative fluconazole induced genes is shown. The values refer to the log2 score of the ratio of RPKM of fluconazole treated over untreated samples. The scale for the heat map is indicated at the bottom and the presence of a SRE is denoted by the solid dot in the lefthand column.

Figure 4. **DNA-binding of Upc2A to SREs in target genes.** A. Locations of SREs from several different promoters are shown. *ERG1*, *CDR1*, *PDR1* and *FKS1* all correspond to the *C. glabrata* locus while Sc*ERG2* is from *S. cerevisiae* and Ca*ERG2* is from *C. albicans*. Note that *ERG1* contains an everted SRE repeat indicated by the arrows. The single SRE is shown in black and white. The extent of DNA protected from cleavage by the DNase I mapping experiment (see below) is shown in gray. B. DNase I protection of the indicated *C. glabrata* promoters is shown. The position of each SRE is indicated by the bar at the righthand side and DNase I hypersensitive sites are noted by the arrows. AG refers to the purine-specific reaction of Maxam-Gilbert chemical sequencing and is carried out on the same radioactive DNA fragment used in the

1028 DNase I reaction. Recombinant Upc2A was added (+) to the DNA probe or omitted (-)
1029 as indicated. C. Electrophoretic mobility shift assay (EMSA) analysis of Upc2A binding
1030 to wild-type and mutant SREs. Biotinylated probes were prepared from the indicated C.
1031 glabrata promoter regions containing either wild-type (wt) or mutant (mut) versions of
1032 each SRE. Sequences of these different SREs are shown at the bottom of the panel
1033 with the altered residues in lower case. The SRE repeats in the *ERG1* promoter are
1034 shown by the divergent arrows at the top of the sequence. Position of the shifted
1035 protein:DNA complexes are shown by the arrows at the lefthand side of each image.
1036 The presence or absence of Upc2A protein is indicated by the (+) or (-), respectively.
1037
1038 Figure 5. **Phenotypes of SRE mutations.** A. Normal expression of *lacZ* gene fusions
1039 requires the presence of intact SREs in Upc2A target promoters. Low-copy-number
1040 plasmids containing translational fusions between *ERG1*, *CDR1* and *PDR1* 5' regulatory
1041 region and *E. coli lacZ* were generated containing either the wild-type version of each
1042 promoter or the same fragment with the SRE mutant (mSRE) shown to reduce in vitro
1043 binding in Figure 4. These plasmids were introduced into wild-type cells, grown in the
1044 absence or presence of fluconazole and then β-galactosidase activity determined. B.
1045 Western blot analysis of *CDR1* and *PDR1* expression upon loss of the wild-type SRE.
1046 All alleles of *PDR1* were integrated into the chromosome while all alleles of *CDR1* were
1047 carried on a low-copy-number plasmid. The presence of either the wild-type (wt) or
1048 mutant (m) SRE at each gene is indicated at the bottom of the panel. Each strain was
1049 grown in the presence or absence of fluconazole and levels of proteins of interest
1050 determined using western blotting with appropriate antibodies as described above.

Erg11 was detected using an anti-peptide antiserum. The right hand panel shows the quantitation as described in Figure 1. C. The strains described above were tested by serial dilution for their growth on rich medium (YPD) or the same medium containing fluconazole (FLC).

Figure 6. **Role for *CDR1* and *PDR1* in anaerobic growth.** A. Wild-type cells were grown under aerobic or anaerobic conditions and total RNA prepared. Levels of the mRNA corresponding to the indicated genes were determined using RT-qPCR. B. Western blot analysis of the indicated proteins was performed using appropriate antisera described earlier. Whole cell protein extracts were prepared after growth in the presence of oxygen (aerobic) or its absence (anaerobic). Quantitation is shown in the right hand panel. C. Expression of *CDR1* and *PDR1* in response to aerobic versus anaerobic growth was assessed by western blotting. Strains containing these genes under control of their wild-type promoter regions or an isogenic strain with both SREs removed from these promoters were used to prepare whole cell protein extracts. Quantitation of at least three western blot experiments is shown on the righthand side of the panel. D. Competitive growth assay between wild-type and *cdr1Δ pdr1Δ* double mutant strains was performed. These two strains were mixed at a starting proportion of 50:50 and then grown in rich medium under aerobic or anaerobic conditions. After growth, the final proportion was determined by plating cells and counting the number of leucine prototrophic colonies (specific for *cdr1Δ pdr1Δ* cells containing *LEU2*).

Figure 7. **Upc2A transcriptionally regulates *FKS1* expression.** A. An isogenic series of strains with the listed *UPC2A* genotypes was tested for resistance to the indicated stress agents that affect the cell wall. Strains were grown to mid-log phase and then serially diluted across each plate. B. Strains containing the different alleles of *UPC2A* were grown and analyzed for levels of the indicated RNAs using RT-qPCR. C. Isogenic wild-type and *upc2AΔ* strains were grown in the presence or absence of caspofungin and levels of *FKS1* and *FKS2* RNA assayed as above. D. A probe from the FKS1 promoter containing the putative SRE shown in Figure 4A was used in a EMSA experiment. A version of this probe lacking the SRE (mSRE) was also compared for its behavior in this assay. Upc2A was either omitted (-) or added (+) to the reaction prior to electrophoresis. E. An *FKS1-lacZ* fusion gene containing either the wild-type or the mSRE version of the promoter was introduced into wild-type cells. Levels of *FKS1*-dependent β-galactosidase were determined in the presence or absence of caspofungin.

1088 Tables

1089

Name	Parent strain	Genotype
KKY2001	CBS138	*his3Δ*::FRT *leu2Δ*::FRT *trp1Δ*::FRT
BVGC3	KKY2001	*ERG11*-3X HA*::his3MX6* KKY2001
BVGC138	BVGC3	*pdr1Δ::loxP* KKY2001
BVGC205	BVGC138	*PDR1::loxP* KKY2001
BVGC207	BVGC138	mSRE *PDR1::loxP* KKY2001
BVGC209	BVGC205	*PDR1::loxP* c*dr1Δ* KKY2001
BVGC213	BVGC207	mSRE *PDR1::loxP* c*dr1Δ* KKY2001
BVGC268	BVGC213	mSRE *PDR1::loxP* c*dr1Δ* KKY2001 *LEU2*
BVGC59	BVGC3	*upc2AΔ* KKY2001
BVGC82	BVGC59	*UPC2A*-3X HA-*UPC2A::loxP* KKY2001
BVGC84	BVGC59	*UPC2A*-3X HA-G898D *UPC2A::loxP* KKY2001
BVGC259	KK2001	*pdr1Δ::loxP cdr1Δ::loxP* KKY2001
BVGC328	BVGC259	*pdr1Δ::loxP cdr1Δ::loxP* KKY2001 *LEU2*

1090

1091 **Table 1.** Strains and relevant genotypes for *C. glabrata* cells used in this study.

Gene	baseMean	log2Fold Change	padj	SRE	Gene	Sc homologue	Function
CAGL0F08965g	39195.9	0.87	6.17E-11	No		MSC7	Orthologs have role in reciprocal meiotic recombination
CAGL0L10714g	38381.7	0.75	3.60E-05	Yes	ERG2	ERG2	C-8 sterol isomerase
CAGL0J03916g	9198.9	0.71	1.54E-06	No	HES1	HES1	Orthologs have oxysterol binding and sterol transport
CAGL0K03927g	10420.4	0.68	0.00029389	No	ERG29	ERG29	Orthologs have role in ergosterol biosynthetic process
CAGL0M07656g	50162.8	0.67	0.00075178	Yes	ERG5	ERG5	Putative C22 sterol desaturase
CAGL0H04081g	49335.7	0.67	0.00075178	Yes	ERG13	ERG13	3-hydroxy-3-methylglutaryl coenzyme A synthase
CAGL0L03828g	8696.4	0.6	0.00493476	Yes	CYB5	CYB5	Orthologs have, role in ergosterol biosynthetic process
CAGL0A00429g	36653.4	0.59	0.00237241	No	ERG4	ERG4	Putative C24 sterol reductase
CAGL0K04455g	236.3	0.52	0.04177062	No		SPR3	Orthologs have role in ascospore formation
CAGL0H04653g	119991.9	0.5	0.0436892	Yes	ERG6	ERG6	C24 sterol methyltransferase
CAGL0L12364g	37830.9	0.5	0.01611664	No	ERG10	ERG10	Orthologs have role in ergosterol biosynthetic process

Table 2. **Genes induced by log2 of 0.5 or greater in the presence of the G898D *UPC2A***. RNA-seq was used to compare the levels of transcripts produced in the presence of the G898D *UPC2A* allele and the ratio of these mRNA levels/those seen in the presence of wild-type *UPC2A* presented as log2 Fold Change.

A.

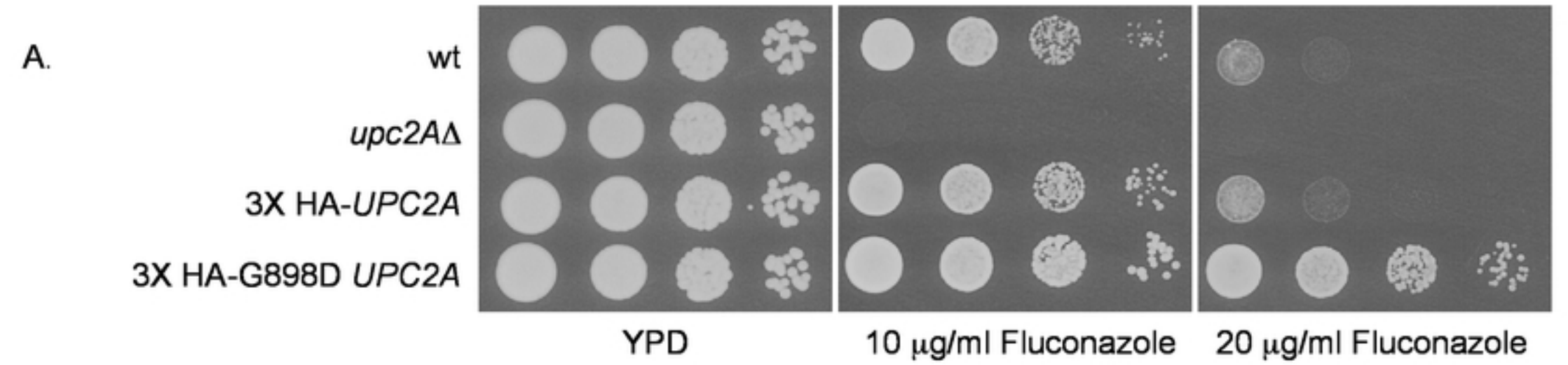

B.

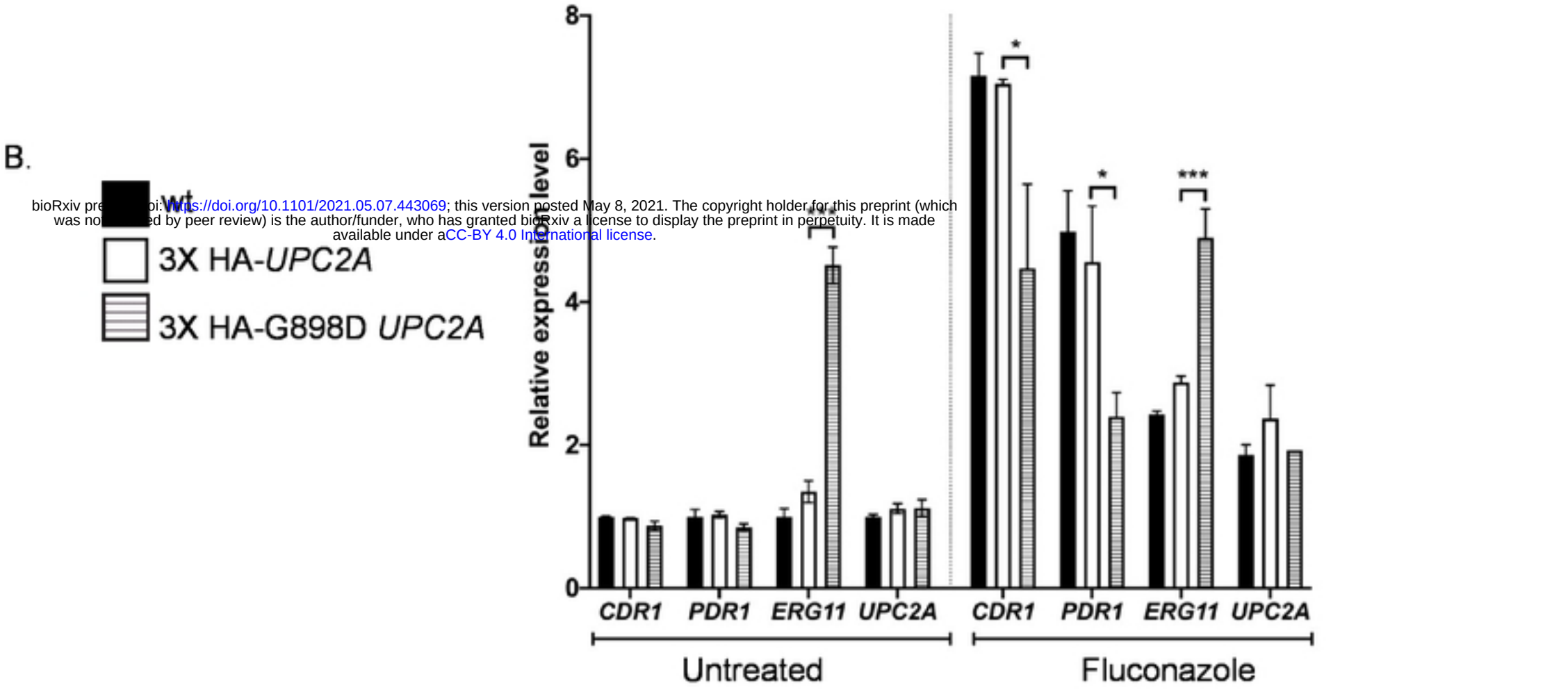

C.

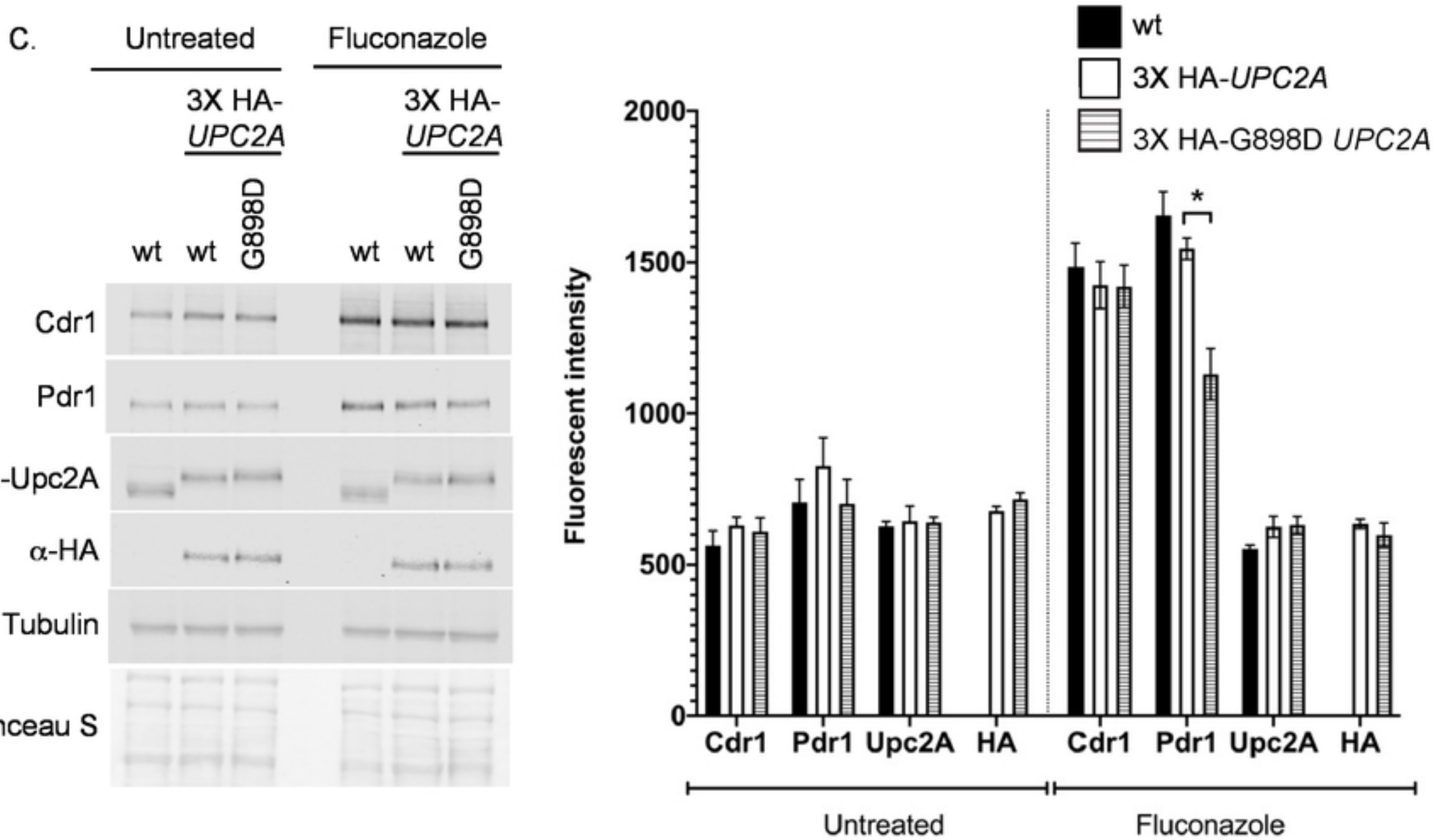

Figure 2. Vu, et al.

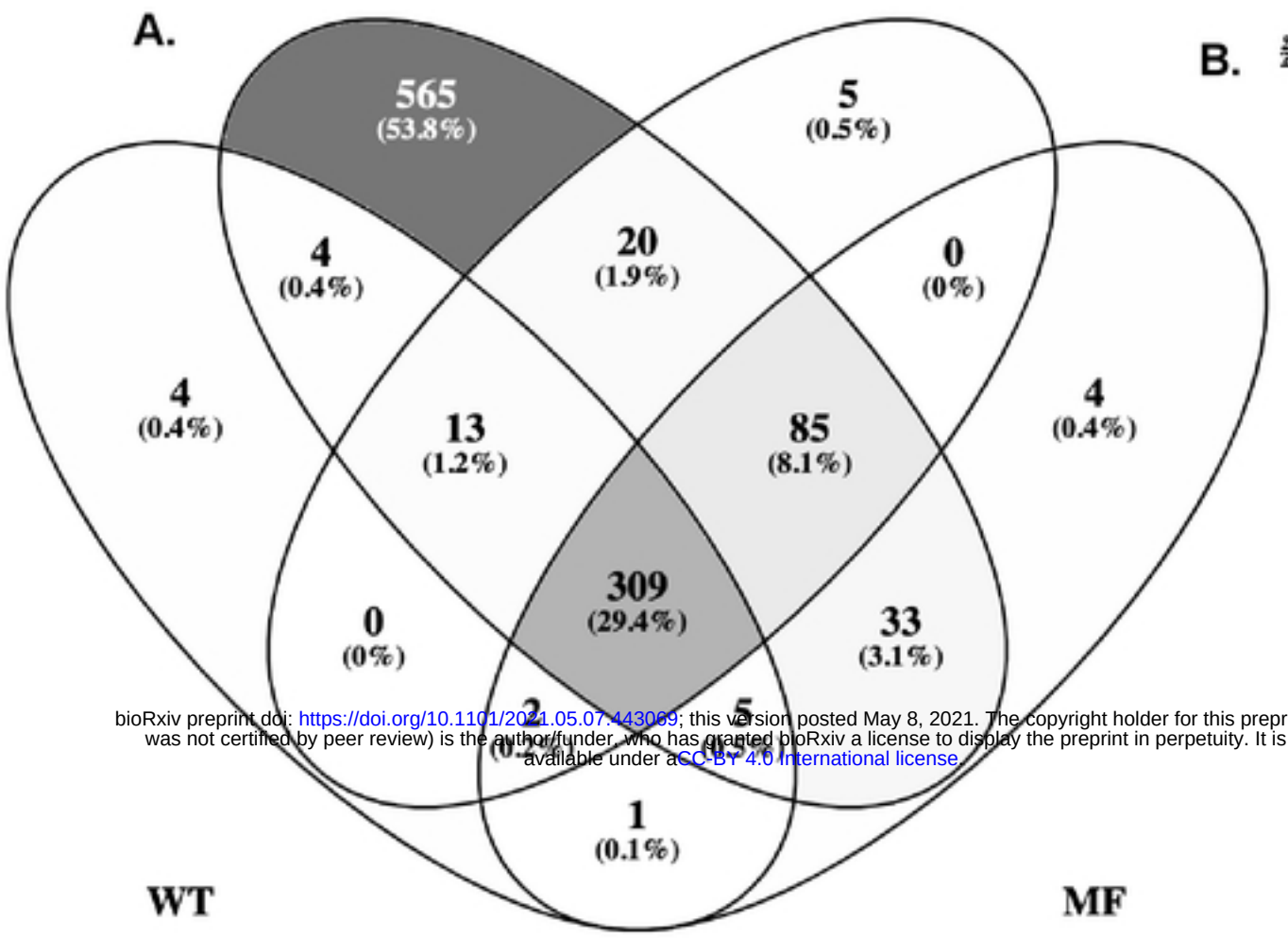

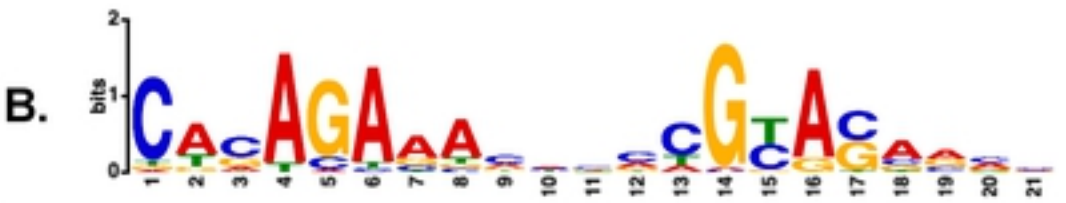

AR1c TCGTATA
AR1b TCGTTTA

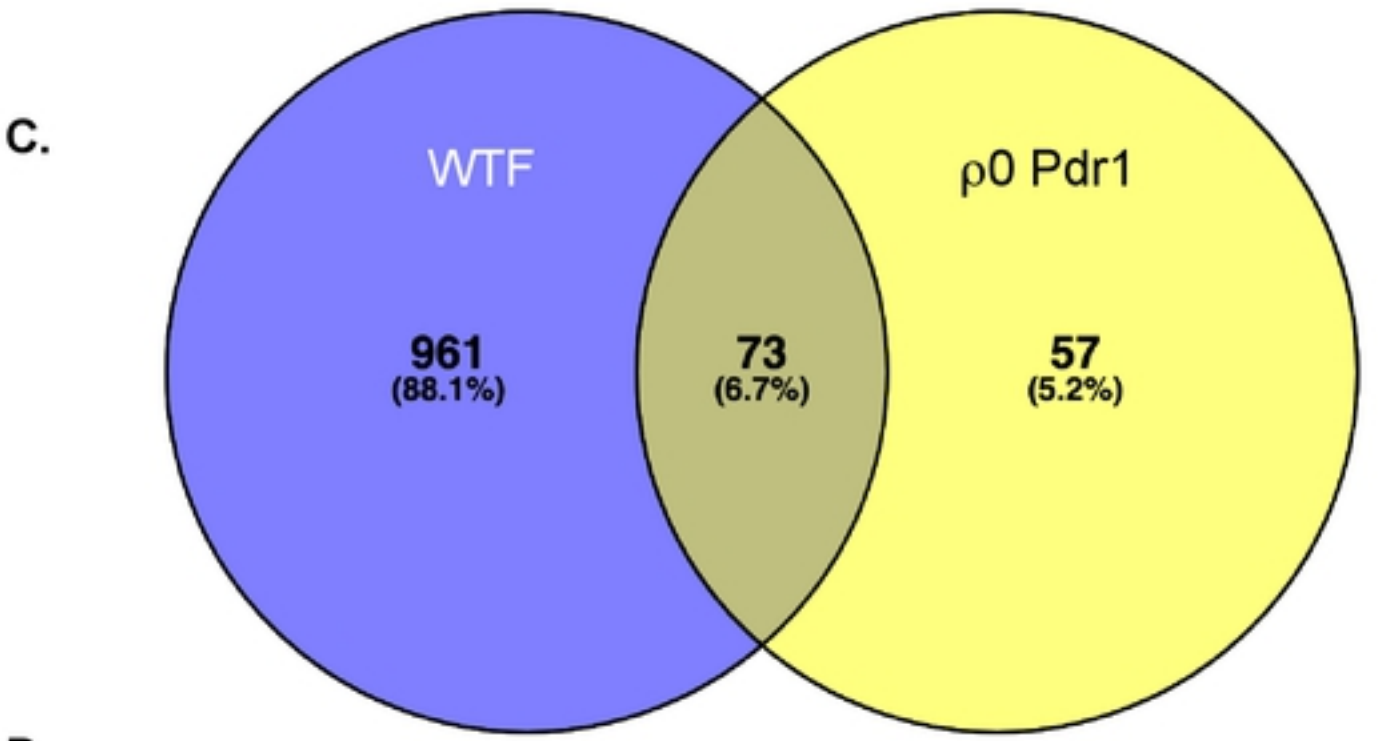

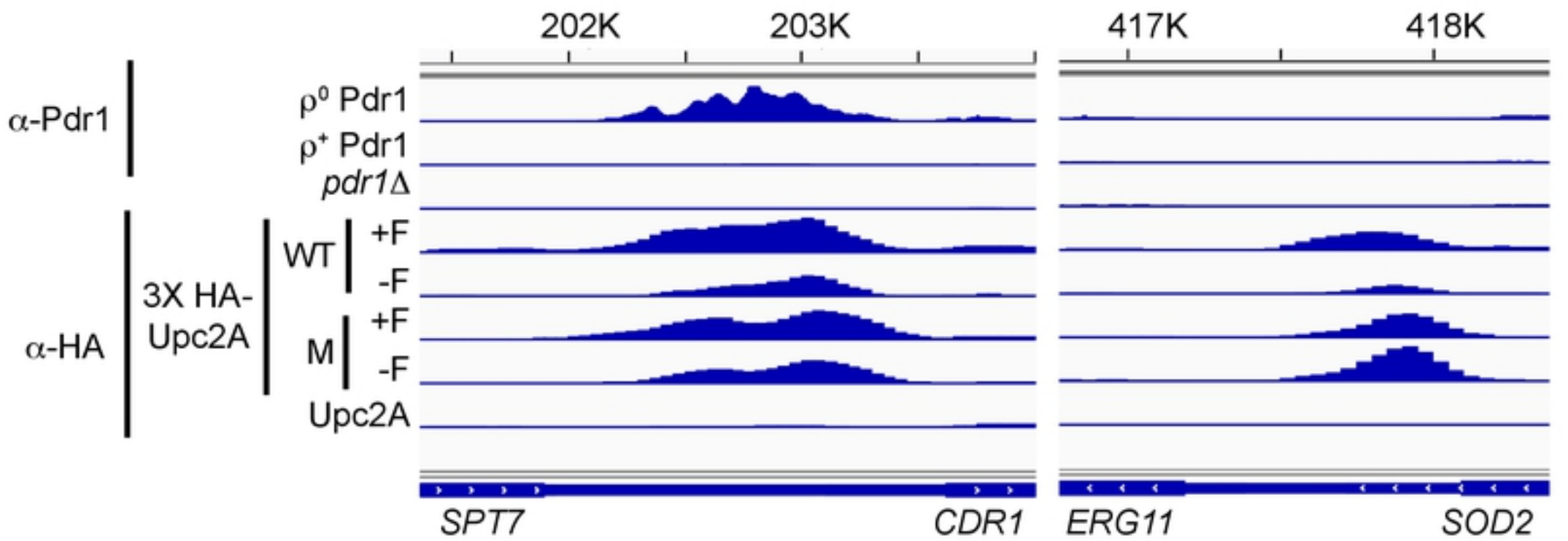

A.

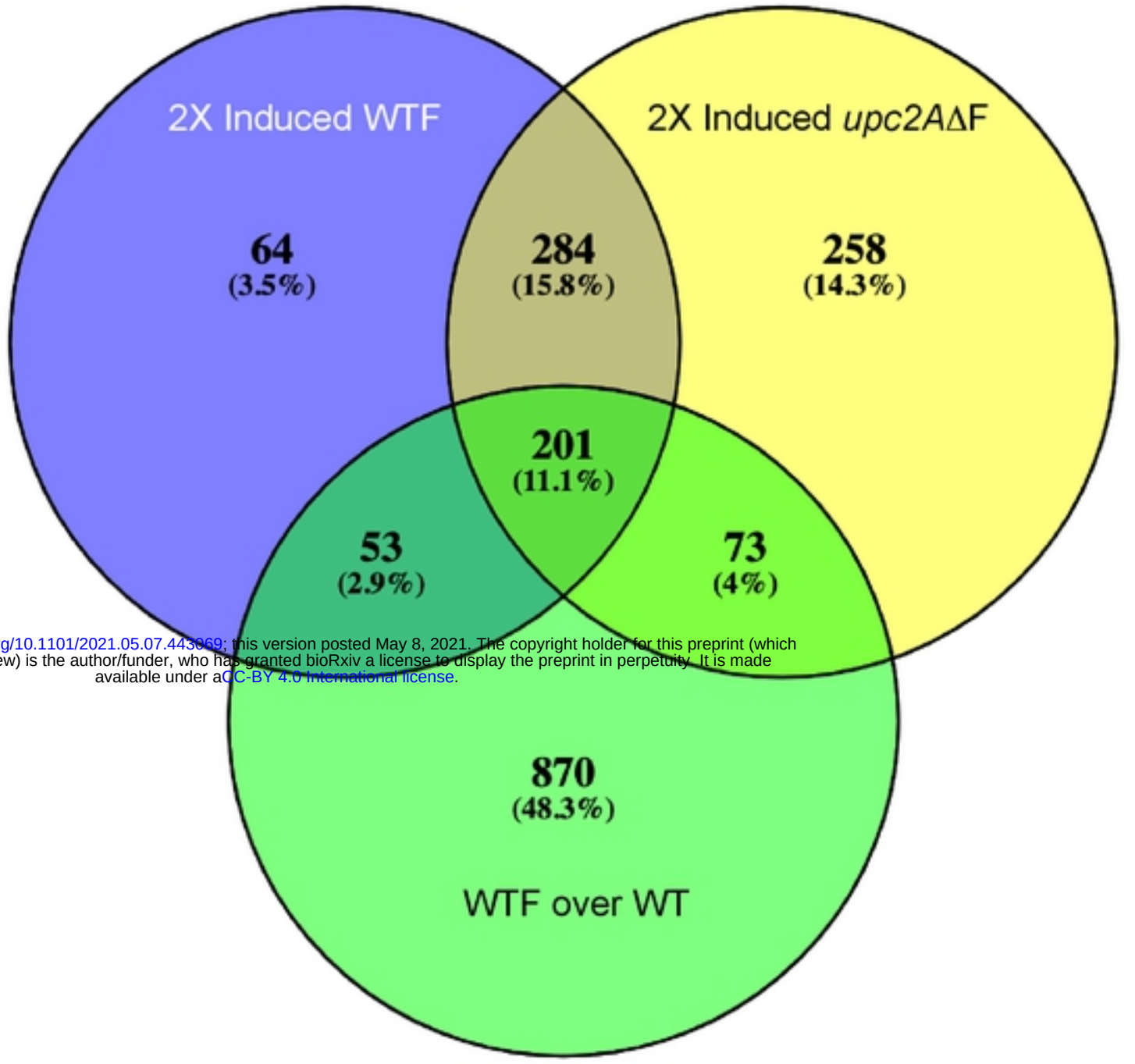

B.

SRE	Log2 FLC wt	Log2 FLC upc2A	Cg	Sc	Product
● CAGL0D05940g	3.6	3.6	ERG1	ERG1	Squalene epoxidase
CAGL0L12364g	0.5	-1.4	ERG10	ERG10	Acetyl-CoA C-acetyltransferase activity
● CAGL0E04334g	1.9	-1.4	ERG11	ERG11	Cytochrome P-450 lanosterol 14-alpha-demethylase
● CAGL0H04081g	0.3	-1.6	ERG13	ERG13	3-hydroxy-3-methylglutaryl coenzyme A synthase
● CAGL0L10714g	2.2	-1.3	ERG2	ERG2	C-8 sterol isomerase
CAGL0L00319g	0.4	-0.9	ERG20	ERG20	Putative farnesyl pyrophosphate synthetase
● CAGL0F01793g	2.6	0.1	ERG3	ERG3	Delta 5,6 sterol desaturase
CAGL0A00429g	1.6	-2.0	ERG4	ERG4	C24 sterol reductase
● CAGL0M07656g	1.2	-0.9	ERG5	ERG5	C22 sterol desaturase
● CAGL0H04653g	0.8	-1.4	ERG6	ERG6	C24 sterol methyltransferase
CAGL0F03993g	0.9	0.7	ERG8	ERG8	Phosphomevalonate kinase
CAGL0M07095g	1.1	-0.3	ERG9	ERG9	Squalene synthase
● CAGL0L11506g	0.1	-1.9	HMG1	HMG1	Hydroxymethylglutaryl-CoA reductase
● CAGL0M01760g	3.6	2.2	CDR1	PDR5	Multidrug transporter of ATP-binding cassette ABC superfamily
● CAGL0F02717g	2.7	0.7	PDH1	PDR15	Multidrug ABC transporter
● CAGL0A00451g	2.2	1.8	PDR1	PDR1	Zinc finger transcription factor
● CAGL0I04862g	1.4	0.4	SNQ2	SNQ2	Multidrug ABC transporter
● CAGL0K00715g	3.4	4.4	RTA1	RTA1	7 transmembrane domain protein
● CAGL0G08624g	0.9	2.1	QDR2	QDR1	Major Facilitator Superfamily transporter
● CAGL0J07436g	-0.2	-1.7	PDR16	PDR16	Phosphatidylinositol transfer protein
● CAGL0L10142g	-1.4	-2.1	RSB1	RSB1	7 transmembrane domain protein

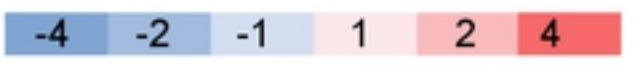

Figure 4. Vu, et al.

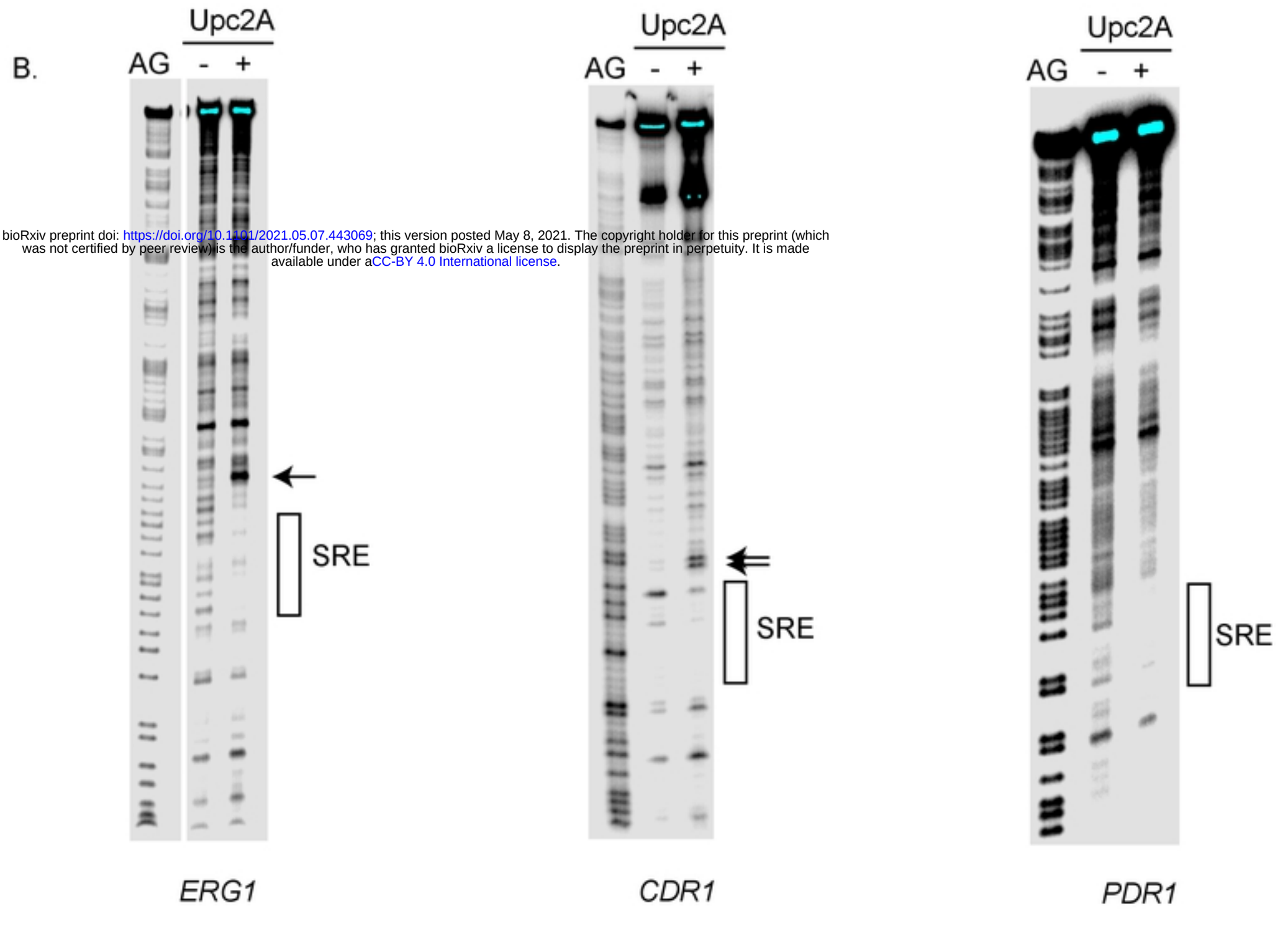

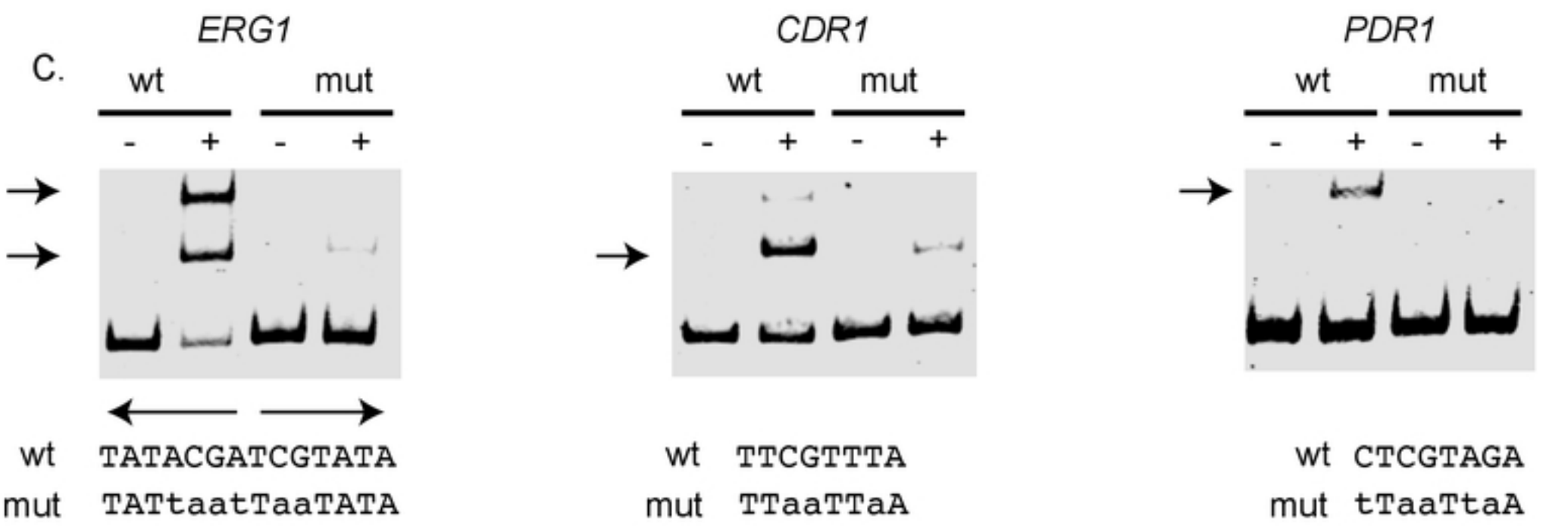

A.

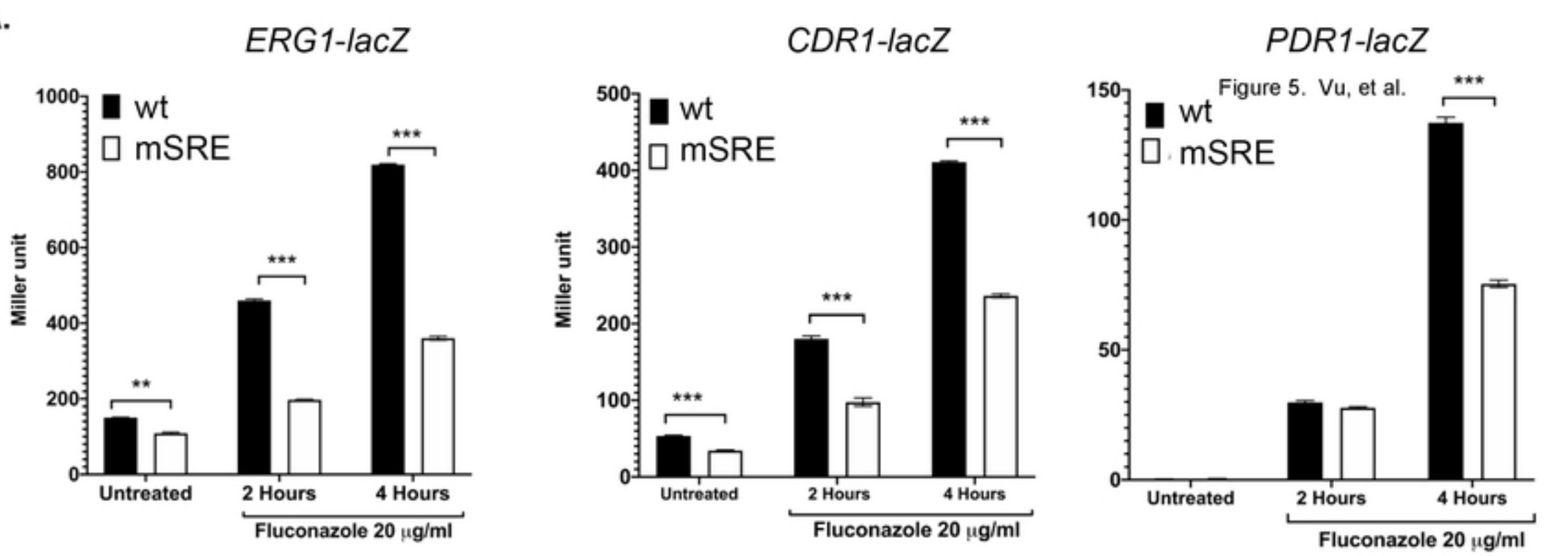

B.

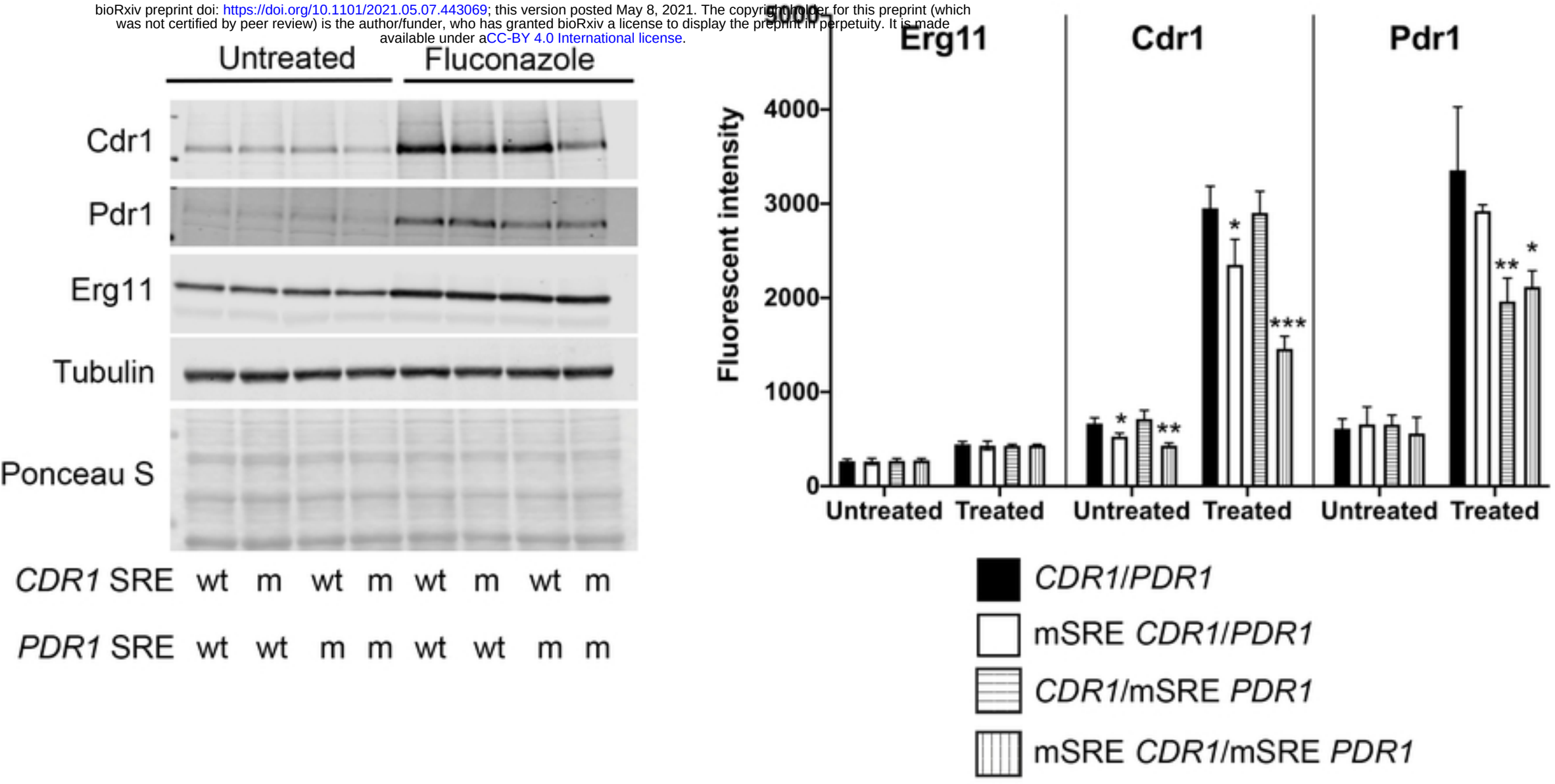

C.

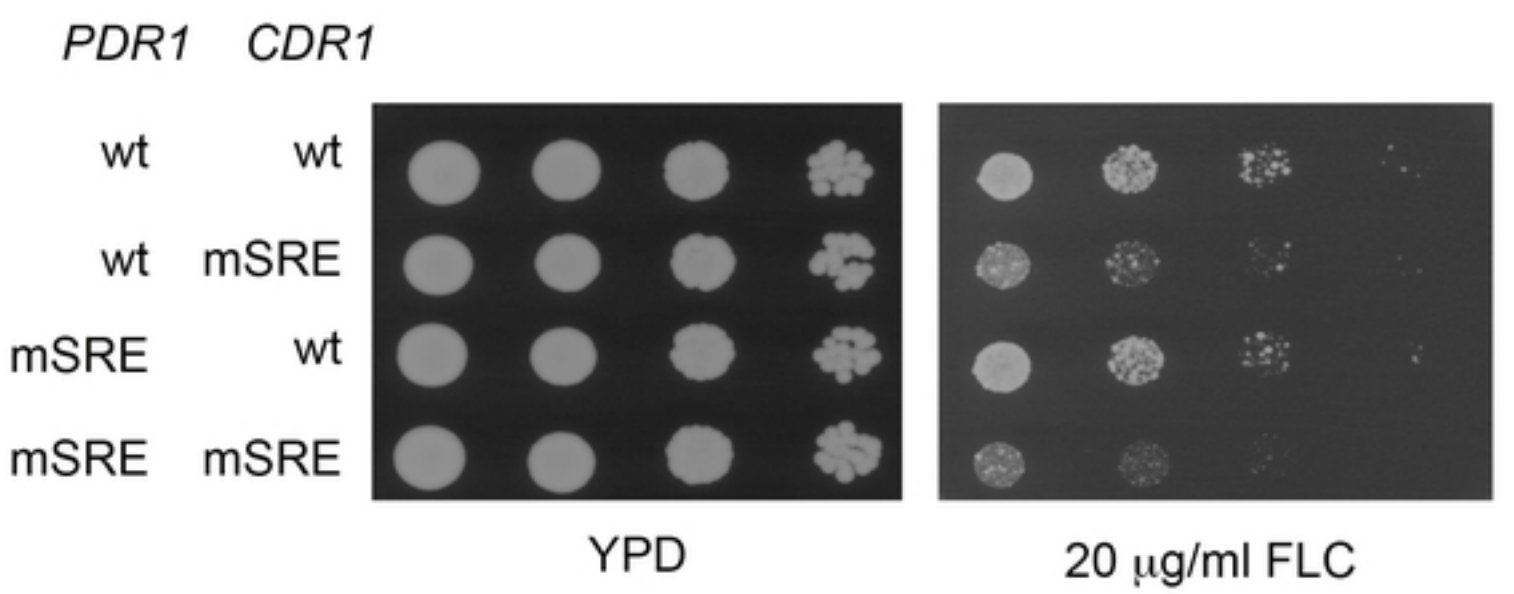

Figure 6. Vu, et al.

A.

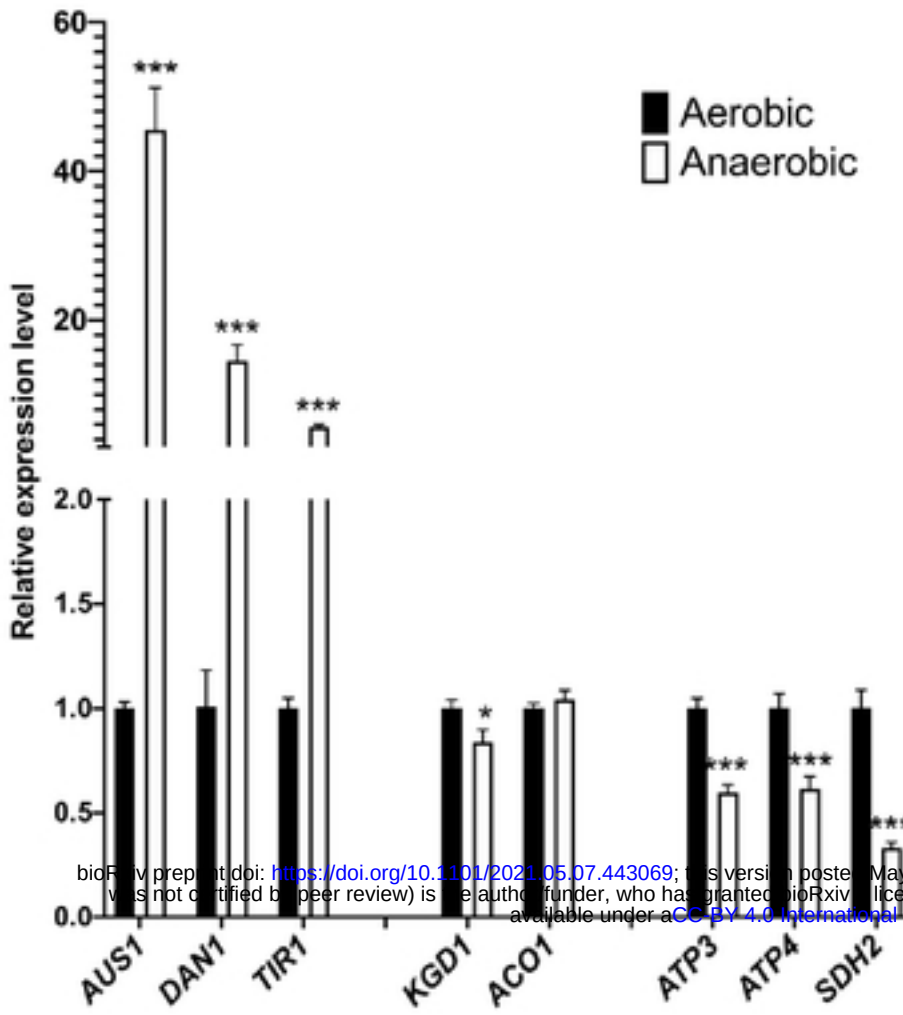

B.

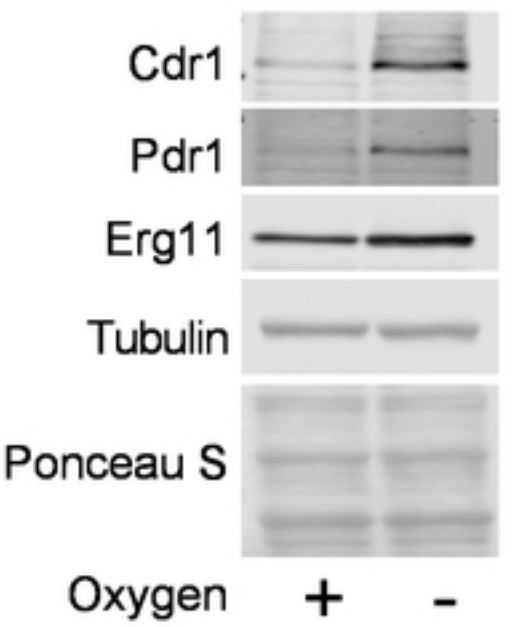

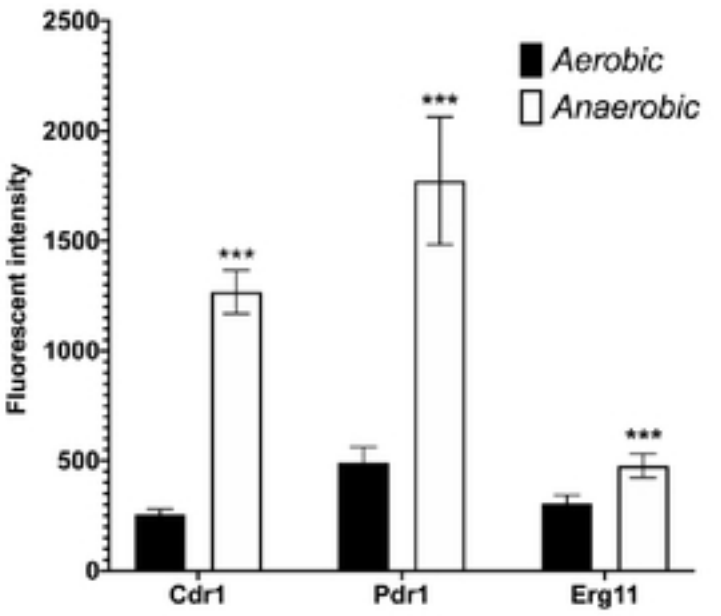

C.

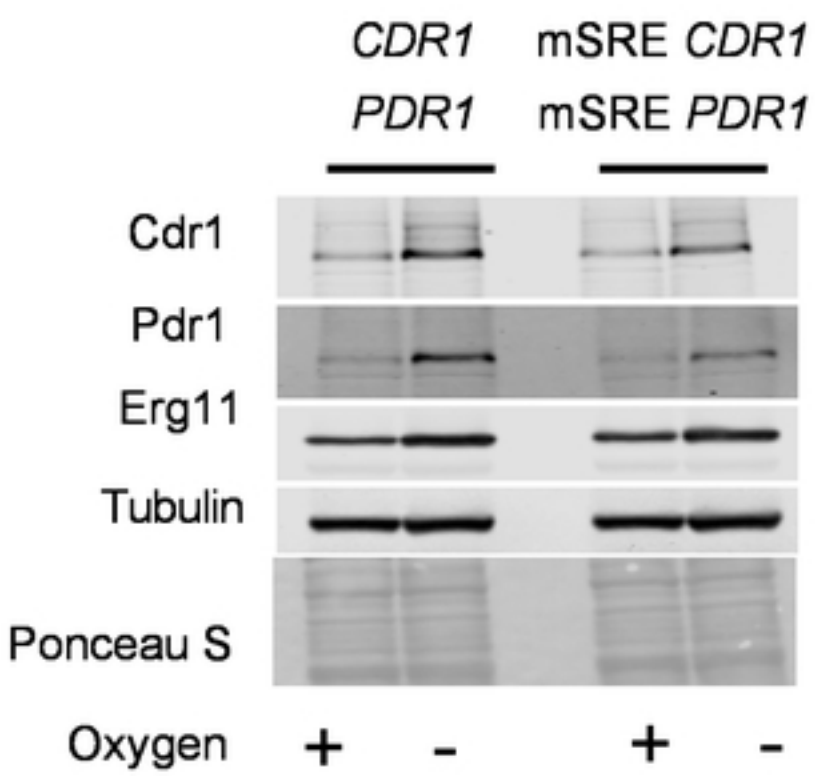

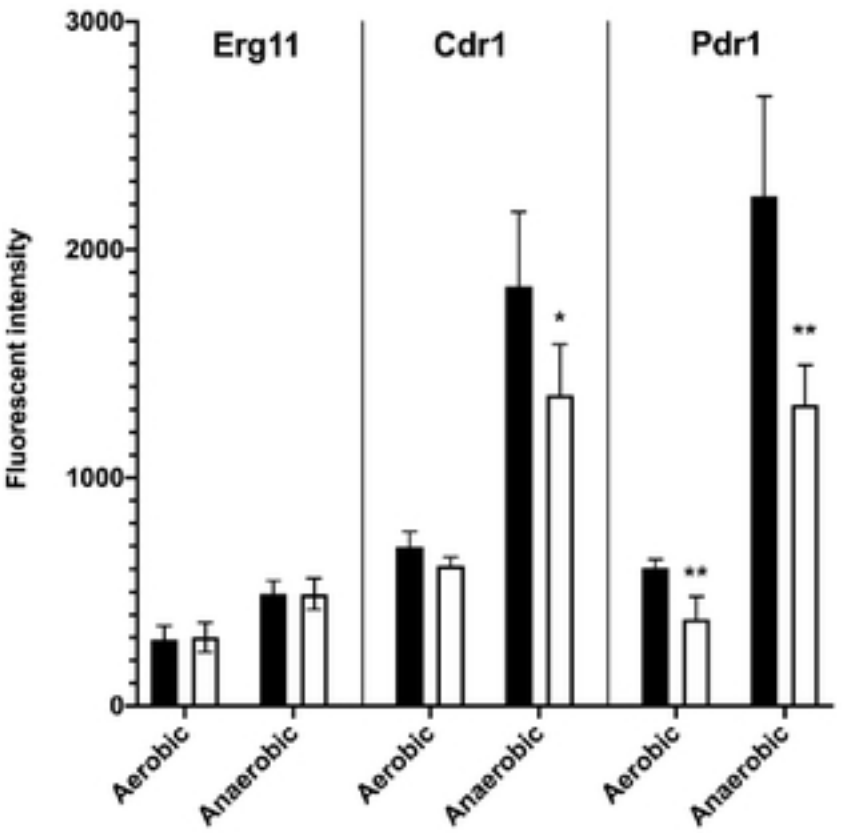

CDR1/PDR1

mSRE CDR1/mSRE PDR1

D.

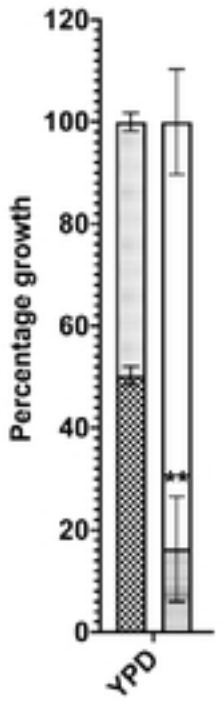

Aerobic WT

Anaerobic WT

Aerobic *pdr1Δ/cdr1Δ*

Anaerobic *pdr1Δ/cdr1Δ*

A.

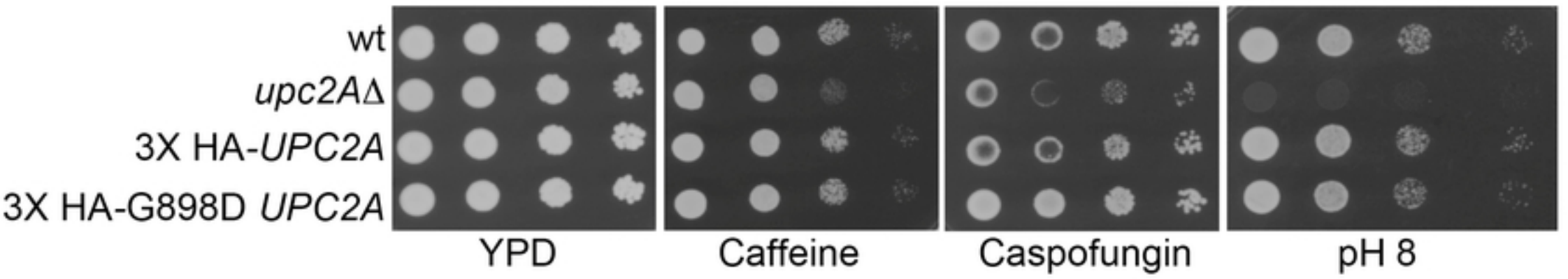

B.

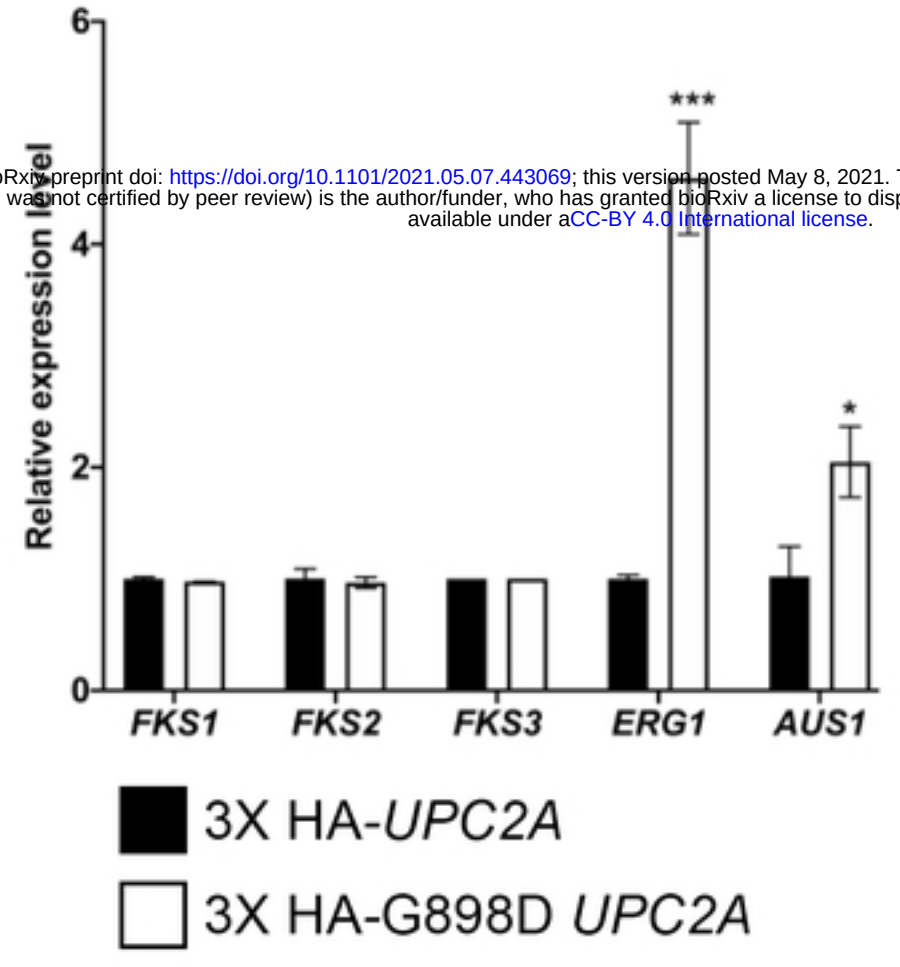

C.

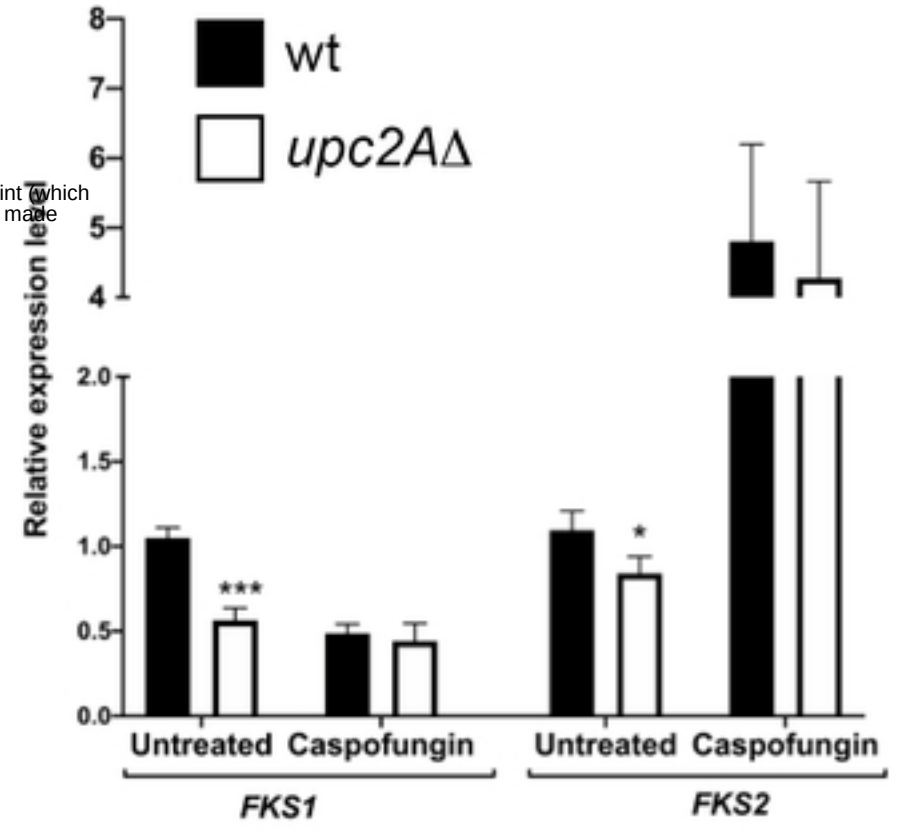

D.

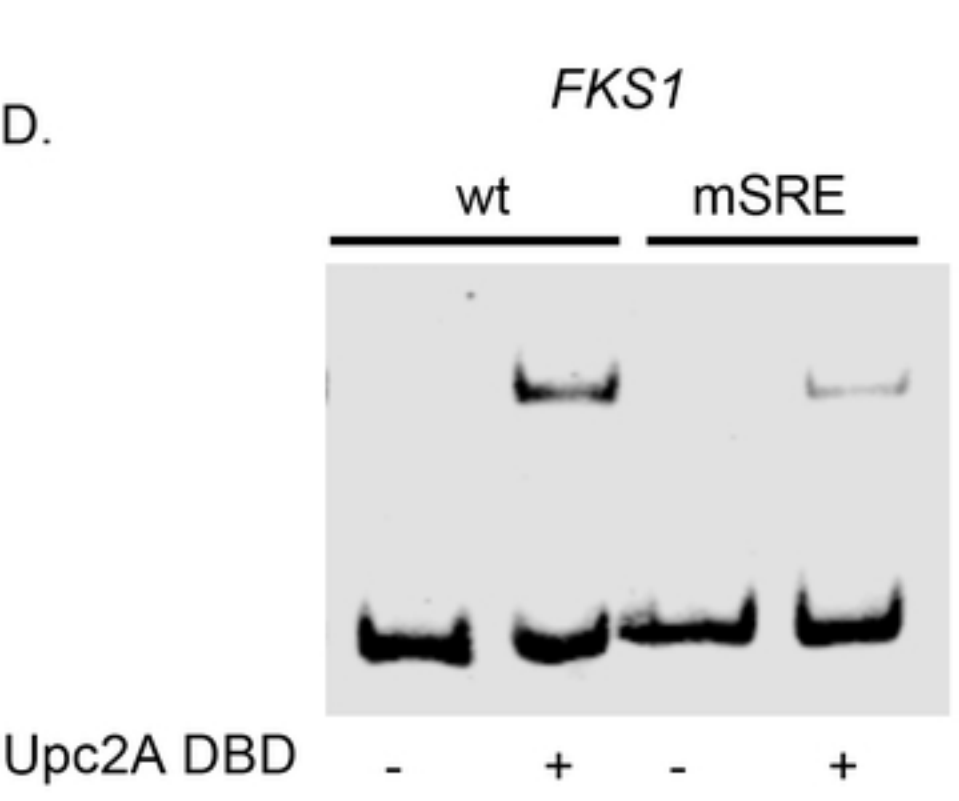

E.